

ADA 086421

LEVEL III

12

30

# CHARACTERIZATION AND ANALYSIS OF INDIUM-DOPED SILICON EXTRINSIC DETECTOR MATERIAL

AD62578

J. Baukus  
Hughes Research Laboratories  
3011 Malibu Canyon Road  
Malibu, CA 90265

T. McGill  
California Institute of Technology  
Pasadena, CA 91125

DTIC  
ELECTE  
JUL 7 1980

April 1980

DAAK-77-C-0082

Interim Technical Report 3

For period 1 July 1978 to 30 June 1979

Approved for public release; distribution unlimited.

Sponsored by  
DEFENSE ADVANCED RESEARCH PROJECTS AGENCY (DoD)  
1400 Wilson Boulevard  
Arlington, VA 22200  
ARPA Order No. 3211, Admendment 333

Monitored by  
Philip R. Boyd  
ATTN: DRSEL-NV-FIR  
NIGHT VISION LABORATORY  
Fort Belvoir, VA 22060

The views and conclusions contained in this document are those of the authors and should not be interpreted as necessarily representing the official policies, either expressed or implied, of the Defense Advanced Research Projects Agency or the U.S. government.

DDC FILE COPY

80 7 2 039

ARPA Order Number	3211, Amendment 3
Name of Contractor	Hughes Aircraft Company
Contract Number	DAAK70-77-C-0082
Effective Date of Contract	31 March 1977
Expiration Date of Contract	30 September 1979
Reporting Period	1 July 1978 through 30 June 1979
Principal Investigator and Phone Number	Dr. Robert Baron (213) 456-6411, Ext. 392
Project Scientist or Engineer and Phone Number	Dr. James Baukus (213) 456-6411, Ext. 336
Short Title of Work	SINDEC (Silicon Indium Material and Detector Characterization)

Accession For	
NTIS <input checked="" type="checkbox"/>	<input type="checkbox"/>
DDC <input type="checkbox"/>	<input type="checkbox"/>
Unannounced Justification	
By _____	
Distribution/	
Availability Codes	
Dist	Avail and/or special
A	

UNCLASSIFIED

SECURITY CLASSIFICATION OF THIS PAGE (When Data Entered)

REPORT DOCUMENTATION PAGE		READ INSTRUCTIONS BEFORE COMPLETING FORM
1. REPORT NUMBER	2. GOVT ACCESSION NO.	3. RECIPIENT'S CATALOG NUMBER
	AD-A086421	(9)
4. TITLE (and Subtitle)		5. TYPE OF REPORT & PERIOD COVERED
CHARACTERIZATION AND ANALYSIS OF INDIUM-DOPED SILICON EXTRINSIC DETECTOR MATERIAL		Interim Report, NO. 3, 1 July 1978 - 30 June 1979
7. AUTHOR(s)		6. PERFORMING ORG. REPORT NUMBER
James F. Baukus and T. McGill		
9. PERFORMING ORGANIZATION NAME AND ADDRESS		8. CONTRACT OR GRANT NUMBER(s)
Hughes Research Laboratories 3011 Malibu Canyon Road Malibu, CA 90265		(15) DAAK70-77-C-0082 ✓ ARPA Order - 3211
11. CONTROLLING OFFICE NAME AND ADDRESS		10. PROGRAM ELEMENT, PROJECT, TASK AREA & WORK UNIT NUMBERS
Defense Advanced Research Projects Agency Arlington, VA 22200		
14. MONITORING AGENCY NAME & ADDRESS (if different from Controlling Office)		12. REPORT DATE
Philip R. Boyd Attn: DRSEL-NV-FIR Night Vision Laboratory Ft. Belvoir, VA 22060		(11) April 1979
16. DISTRIBUTION STATEMENT (of this Report)		13. NUMBER OF PAGES
Approved for public release; distribution unlimited.		65 (42/59)
17. DISTRIBUTION STATEMENT (of the abstract entered in Block 20, if different from Report)		15. SECURITY CLASS. (of this report)
		UNCLASSIFIED
18. SUPPLEMENTARY NOTES		15a. DECLASSIFICATION DOWNGRADING SCHEDULE
19. KEY WORDS (Continue on reverse side if necessary and identify by block number)		
Extrinsic silicon, Infrared detectors, SIMDEC program, Photoluminescence, Excitons, IR, Capture cross section		
20. ABSTRACT (Continue on reverse side if necessary and identify by block number)		
This third report of a two-year program describes progress made in analyzing Si:In detector material. Hall-effect, photoluminescence, and IR measurements were performed to characterize the X level and to determine its nature.		

DD FORM 1 JAN 73 1473

EDITION OF 1 NOV 65 IS OBSOLETE

UNCLASSIFIED

SECURITY CLASSIFICATION OF THIS PAGE (When Data Entered)

172600

bpg

# TABLE OF CONTENTS

SECTION		PAGE
	LIST OF ILLUSTRATIONS . . . . .	5
1	INTRODUCTION AND SUMMARY . . . . .	7
2	CRYSTAL GROWTH AND CHARACTERIZATION . . . . .	9
	A. Crystal Growth and Analysis . . . . .	9
	B. IR Spectroscopic Studies . . . . .	13
	C. Charged-Particle Activation Analyses for O and C . . . . .	14
	D. Ion Implantation of In and C . . . . .	16
	E. FZ and Czo Anneal Studies . . . . .	18
3	PHOTOLUMINESCENCE STUDIES IN EXTRINSIC SILICON . . . . .	25
	A. Observation of Long-Lived Lines in Si:In: the P, Q and R Lines . . . . .	25
	B. Evidence for Jahn-Teller Splitting of the Ground State of Si:In . . . . .	28
	C. Search for Photoluminescence from the X Level . . . . .	30
	D. Excitation Transfer . . . . .	30
	REFERENCES . . . . .	45
	APPENDIX A - Nature of the 0.111-eV Acceptor Level in Indium-Doped Silicon . . . . .	47
	APPENDIX B - Observation of Long Lifetime Lines in Photoluminescence from Si:In . . . . .	53
	APPENDIX C - Evidence for an Excited Level of the Neutral Indium Acceptor in Silicon . . . . .	61

# LIST OF ILLUSTRATIONS

FIGURE		PAGE
1	The ratio of X-level concentration to In concentration versus the O and C concentrations . . . . .	15
2	X-level and donor concentrations as functions of anneal temperature for crystal Z008 . . . . .	23
3	X-level and donor concentrations as functions of anneal temperature for crystal C019 . . . . .	24
4	A representative photoluminescence spectrum for indium-doped Si . . . . .	26
5	The photoluminescence spectra from several Czochralski-grown, indium-doped Si samples . . . . .	27
6	A schematic of the energy levels on a neutral indium . . . . .	29
7	The intensity of the bound exciton (BE) due to boron in the TO-phonon replica as a function of pump power . . . . .	37
8	The intensity of the bound exciton (BE) due to indium in the no-phonon replica as a function of pump power . . . . .	38
9	The ratio $I_{B_{In}}^O / N_B I_{In}^{NP}$ as a function of $N_{In}$ . . . . .	40
10	The photoluminescence spectra of two samples: Z20601A and C112M . . . . .	42

## SECTION 1

### INTRODUCTION AND SUMMARY

The objective of the silicon indium material and detector characterization (SIMDEC) program being conducted by Hughes under contract DAAK70-77-C-0082 is to investigate the nature of defects in indium-doped silicon detector material and to develop techniques for the control of quality in the growth of extrinsic and high-purity undoped silicon for IR detector monolithic chips. The discovery at Hughes<sup>1</sup> of a second, shallower acceptor level in indium-doped silicon (Si:In), the so-called X level, demonstrated the need for further research on Si:In. The X level has been observed in measurements of Hall effect versus temperature and of IR photoconductivity<sup>1,2,3</sup> and absorption.<sup>4</sup> It is undesirable in extrinsic Si:In photoconductors because its shallower energy level results in excess thermally ionized carriers. These lower the maximum temperature at which background-limited detectivities can be obtained. This can reduce the operating temperature by as much as 10°K with a corresponding increase in cooling power requirements.

The X level has an ionization energy of 0.11 eV and has a concentration that is a direct function of the concentration of the indium. Different growth conditions can produce drastically different amounts of X level in comparably indium doped material samples. Thus, it cannot be a discrete dopant. These facts indicate that the X level is likely to be a complex of indium and some other crystalline defect or impurity. However, the exact physical nature of the X level was unknown at the beginning of the program, as were the growth and processing factors that determine its concentration. The purpose, then, of the SIMDEC program has been to apply the appropriate physical measurements to Si:In to identify the nature of the X level and means of controlling it.

The prime contractor for this program is Hughes Research Laboratories (HRL); the California Institute of Technology (CIT) is the subcontractor.

The most significant result during this reporting period was the discovery of the nature of the X level in Si:In. The X level was found to be an indium-carbon nearest-neighbor pair. This model was established on the basis of X level and In data (taken by Hall-effect measurements) and carbon data (from IR transmission studies).

The X-level concentration observed as a function of anneal temperature for Czochralski (Czo) crystals is consistent with the mass-action law and yields a reasonable In-C pair binding energy, as first observed and reported by our group.<sup>5</sup> A reprint of our paper is included as Appendix A.

The results of studies carried out at HRL are contained in Section 2. Six additional crystals were grown for the program during this period. The results of Hall-effect analysis for samples from these and other related crystals are presented. The concentrations of In, O, and C obtained from IR transmission data are discussed. Eighteen additional samples were evaluated during this period in order to confirm the model and extend the range of applicability of the data. Ion-implantation and anneal studies to confirm the X-level model are described, as is an IR&D-funded investigation of an alternative method of measurement of O and C that promises higher sensitivity.

The progress at CIT during this period is described in Section 3. The origin of four photoluminescence lines observed uniquely in Si:In has been determined. Three of the lines are due to an isoelectronic trap (or traps), and the fourth arises from Jahn-Teller splitting of the neutral indium ground state due to the indium atom being slightly away from its lattice site. A thorough investigation was made into the problem of the detection of background impurities and defects at concentrations substantially below that of the majority dopant.

The appendices are reprints of refereed papers published in the open literature during this reporting period.

## SECTION 2

### CRYSTAL GROWTH AND CHARACTERIZATION

This section describes progress at HRL during the reporting period. Six crystals were grown and analyzed, and samples from these and other crystals were analyzed and delivered to CIT for photoluminescence analysis. Continued IR spectroscopic studies verified the X-level model. A related, IR&D-funded project on charged particle activation analysis is described as are ion implantation and anneal studies on the X level in Si:In.

#### A. CRYSTAL GROWTH AND ANALYSIS

Six crystals were grown specifically for the SIMDEC program during this reporting period. Five Czo crystals and one float-zone (FZ) crystal were grown: two were not intentionally doped, one was In doped, and three were doped with both In and B. Hall-effect measurements versus temperature were made on samples from all five crystals.

In addition, most of the crystals were analyzed for O and C by IR spectroscopy. These results are summarized in Table 1.

Crystal C078, grown by the Czo method, was undoped. It was grown to determine if the C was introduced by the In dopant charge. Since no dopant was added in this growth, the amount of B and P picked up from this Suprasil-lined crucible could also be determined.

The crystal had a C concentration slightly above  $10^{17} \text{ cm}^{-3}$ , which ranked it with the more heavily C-contaminated crystals. Thus, the In charge was clearly not the source of the carbon associated with the X level in Si:In. The Hall results indicated P at  $8.3 \times 10^{13} \text{ cm}^{-3}$  at the tang. The p-type compensation, presumably B, rose slightly from 5.0 to  $5.4 \times 10^{13} \text{ cm}^{-3}$  from seed to tang. This increase corresponds to 3.3 ppb of B in the crucible. This is a rather low value, but within the lot-to-lot variation observed for the Suprasil crucible material.

An attempt was made to minimize C contamination from the grower components and dopant charge in crystal C086. Before growth was initiated, the heater radiation shields, Suprasil-lined crucible, and

Table 1. Results of Hall-Effect and IR Absorption Measurements of SIMDEC-Related Crystals

Ingot	Position	$N_{In}^+$ $cm^{-3}$	$N_{X}^+$ $cm^{-3}$	$N_{B}^+$ $cm^{-3}$	$N_{D}^+$ $cm^{-3}$	$n_{In}^+$ $cm^{-1}$	$\sigma_{In}^+$ $\times 10^{-17} cm^2$	$N_{O}^+$ $cm^{-3}$	$N_{L}^+$ $cm^{-3}$
C017	TANG	$3.8 \times 10^{17}$	$3.4 \times 10^{15}$	-	$1.3 \times 10^{14}$	LARGE	-	$1.4 \times 10^{18}$	$4.8 \times 10^{16}$
C025	SEED	$1.5 \times 10^{17}$	$7.3 \times 10^{14}$	-	$4.8 \times 10^{13}$	10.0	6.7	$1.3 \times 10^{18}$	$4.0 \times 10^{16}$
	MID	$1.6 \times 10^{17}$	$9.3 \times 10^{14}$	$2.6 \times 10^{13}$	$2.3 \times 10^{13}$	12.8	8.0	$8.8 \times 10^{17}$	$1.1 \times 10^{17}$
C049	SEED	$8.8 \times 10^{16}$	$1.2 \times 10^{15}$	-	$1.3 \times 10^{14}$	8.1	9.2	$1.4 \times 10^{18}$	$1.1 \times 10^{17}$
C042	TANG	$3.0 \times 10^{15}$	$5.8 \times 10^{13}$	-	$6.1 \times 10^{13}$	SMALL	-	$1.3 \times 10^{18}$	$3.6 \times 10^{16}$
C078	SEED			$5.0 \times 10^{13}$	$8.3 \times 10^{13}$			$8.8 \times 10^{17}$	$1.1 \times 10^{17}$
	TANG			$5.4 \times 10^{13}$	$1.1 \times 10^{14}$				
C086	SEED	$1.1 \times 10^{17}$	$3.2 \times 10^{14}$	-	$1.3 \times 10^{13}$			$3.0 \times 10^{17}$	$3.0 \times 10^{16}$
	TANG	$1.4 \times 10^{17}$	$4.0 \times 10^{14}$	-	$2.2 \times 10^{13}$				
C097	TANG			$3.8 \times 10^{14}$	$3.6 \times 10^{14}$			$5.1 \times 10^{17}$	$1.3 \times 10^{17}$
C112	MID	$3.4 \times 10^{17}$	-	$4.5 \times 10^{15}$	$3.6 \times 10^{14}$			$1.0 \times 10^{18}$	
C117	SEED	$2.1 \times 10^{16}$	$5.0 \times 10^{14}$	$7.8 \times 10^{13}$	$2.2 \times 10^{13}$	1.83	8.7	$8.4 \times 10^{17}$	$2.0 \times 10^{17}$
C20102A	650/60	$6.0 \times 10^{16}$	$5.2 \times 10^{14}$	-	$9.0 \times 10^{13}$	6.6	11.0	$1.0 \times 10^{18}$	$3.4 \times 10^{16}$
C20102B	850/60	$6.1 \times 10^{16}$	$1.1 \times 10^{14}$	-	$1.1 \times 10^{14}$	6.6	10.8	$8.6 \times 10^{17}$	$4.1 \times 10^{16}$
C70401	TANG	$1.8 \times 10^{17}$	$1 \times 10^{14}$	$1.9 \times 10^{14}$	$7.0 \times 10^{13}$	14.2	7.9	$3.9 \times 10^{17}$	$8.3 \times 10^{15}$
C74101	SEED			$5.3 \times 10^{13}$	$1.3 \times 10^{13}$			$9.7 \times 10^{17}$	$1.0 \times 10^{16}$
1001	TANG			$1.1 \times 10^{14}$	$2.6 \times 10^{13}$			$6.7 \times 10^{17}$	$1.6 \times 10^{17}$
Z0088	SEED(B)	$1.0 \times 10^{17}$	$1.8 \times 10^{14}$	-	$8.8 \times 10^{12}$			-	$2.0 \times 10^{16}$
Z059	SEED	$8.4 \times 10^{14}$	$7.0 \times 10^{11}$	$1.6 \times 10^{13}$	$1.0 \times 10^{13}$				
Z074	SEED	$1.7 \times 10^{16}$	$4.2 \times 10^{13}$	$3.9 \times 10^{13}$	$2.0 \times 10^{13}$	1.9	11.6	-	$6.8 \times 10^{16}$
Z076	MID			$\approx 4 \times 10^{12}$	$2.1 \times 10^{13}$			-	$2.7 \times 10^{15}$
Z111	SEED			$5.0 \times 10^{12}$	$3.1 \times 10^{12}$			-	$1.6 \times 10^{16}$
Z7577	M/P							-	-

7024

crucible holder components were baked out under vacuum to remove any volatile contaminants. The In dopant charge was separately vacuum baked and then recleaned, as was the crucible.

The resulting ingot was lower in X level than other comparably doped Si:In crystals grown in the small (1 kg) pullers, but still substantially larger than crystals from the large (3 kg) grower. These experiments point very clearly to the graphite heater, radiation shields, and crucible holder as sources of the carbon. The definitive experiment would be to grow a Si:In crystal in a small grower with no graphite components. We attempted to procure tungsten components for use in our system, but the vendor was not willing to supply parts adapted to our grower.

An undoped crystal, F001, was grown in an rf-heated growth apparatus to avoid contamination from a graphite heater. However, the system required a graphite susceptor to initiate meltdown, and the resulting crystal had a high C content.

Three crystals were grown specifically for the CIT excitation transfer experiment. All were double doped with In and B. Crystals C112 and C117 were grown by Czo, while Z163 was a FZ pass given to a Si:In Czo crystal, C004. It was anticipated that this FZ pass would reduce the In concentration by more than three orders of magnitude and also greatly reduce the P concentration. The Hall-effect measurement results for both Z163 and C004 are listed in Table 2. The In concentration declined, as expected, while the B concentration, which had been expected to remain constant, increased slightly. The net donor concentration was reduced by less than a factor of 2. The resulting levels of B and donors are probably the result of contamination. However, these crystals were satisfactory for the CIT experiment.

In addition to samples from these crystals, samples from several crystals not grown specifically for the SIMDEC program were delivered to CIT for photoluminescence studies. Hall-effect versus temperature data were measured and analyzed so as to provide CIT with well-characterized samples. The Hall analyses for samples from crystals C71601, C008, and C014 were given in the SIMDEC Interim Technical Report #2.<sup>6</sup> The results for samples from crystals Z074, C74101, C025 and C20102 are given in Table 1.

Table 2. Dopant Concentrations of Crystals

C004 and Z163

Crystal	Position	$N_{In},$ $cm^{-3}$	$N_X,$ $cm^{-3}$	$N_B,$ $cm^{-3}$	$N_D,$ $cm^{-3}$
C004	MIDDLE	$2.0 \times 10^{16}$	$2.9 \times 10^{13}$	$2.8 \times 10^{13}$	$1.5 \times 10^{13}$
Z163	SEED	$6.8 \times 10^{12}$	-	$3.5 \times 10^{13}$	$8.8 \times 10^{12}$
	TANG	$2.2 \times 10^{13}$	-	$3.9 \times 10^{13}$	$1.0 \times 10^{13}$

7024

## B. IR SPECTROSCOPIC STUDIES

IR spectral measurements of silicon samples grown under various conditions were continued during this reporting period to determine the O and C content of the crystals and the relationship, if any, of these impurities to the X-level concentration. A correlation between In concentration and X-level concentration has been reported by us<sup>1</sup> and substantiated by others.<sup>2-4</sup> However, since samples grown under different conditions with similar In concentrations showed differences in the X-level concentration, it seemed unlikely that the X level was a simple In complex. At least one more component appeared to be necessary. The IR measurements identified this component as C and enabled the establishment of a model of the X level as an indium-carbon substitutional nearest-neighbor pair. This result, which is the most significant result of the SIMDEC program, has been published in Applied Physics Letters.<sup>5</sup> A reprint of this paper is included as Appendix A.

The experimental arrangement has been described in the previous report.<sup>6</sup> During this period, the sample and window holders were modified to enable them to be changed more readily. The windows were subsequently changed to KCl, which is much less hygroscopic than the previously used CsI.

As indicated in the previous report, the absorption coefficients for O and C were calculated from the peak of their respective absorption curves. These results were also plotted in terms of the peak-half-width product, which approximates the area of the absorption line. The data were consistent; thus, we have continued to use the peak value since the same instrument slit program is used for all these measurements, and the measured resolutions of the line were always very nearly the same.

The measurements made during this period are summarized in Table 1, which contains the O and C concentrations calculated from the IR as well as the In, X-level, B, and donor concentrations as appropriate when these values could be calculated from Hall-effect data on adjacent samples. The Czo Hall-effect samples were annealed at 650°C for 30 min

to reduce the O donor concentration; the optical samples were not annealed. The samples measured represent a range of In concentrations of two orders of magnitude, X-level concentrations of about one order, and C concentrations of about two orders. The O concentration was either near  $1.0 \times 10^{18} \text{ cm}^{-3}$  or below the detection limit of  $1.0 \times 10^{15} \text{ cm}^{-3}$ , depending on whether the sample was from a Czo or an FZ crystal.

Table 1 also contains the In absorption coefficient as calculated from the IR spectra and the absorption cross section based on the corresponding  $N_{\text{In}}$  value. Also included are O and C concentrations for several undoped crystals, also measured by IR transmission.

Figure 1 is a plot of the X to In concentration ratio versus  $N_{\text{O}}$  and  $N_{\text{C}}$ . The plot shows a correlation with the C data and clearly no correlation with O; note that the FZ  $N_{\text{O}}$  values are less than  $1.0 \times 10^{15} \text{ cm}^{-3}$ . The curve in the figure is a unit-slope straight line, as predicted by the mass action law. This gives a reasonably good fit considering the uncertainties in determining the three concentrations involved over this wide a range of parameters.

#### C. CHARGED-PARTICLE ACTIVATION ANALYSES FOR O AND C

A separate IR&D study was performed, under contract with HRL by Prof. R. Hart at Texas A&M University, to investigate a new method of analysis for O and C in Si. This work is described here because correlations were made with samples measured by IR absorption in the SIMDEC program and because this technique holds out the promise of better sensitivity for detecting O and C.

Charged-particle activation analysis (CPAA) involves bombarding the Si sample with high-energy  $^3\text{He}$  and D beams for O and C, respectively. The reactions are  $^{16}\text{O}(^3\text{He},n)^{18}\text{F}$  and  $^{12}\text{C}(D,n)^{13}\text{N}$ . The activities of the isotopes of F or N are then analyzed to determine the amount of O or C present in the sample. This work is in its early stages, and thus improvements are still being made in beam current magnitude and its measurement, sample mounting procedure, counting technique, and the

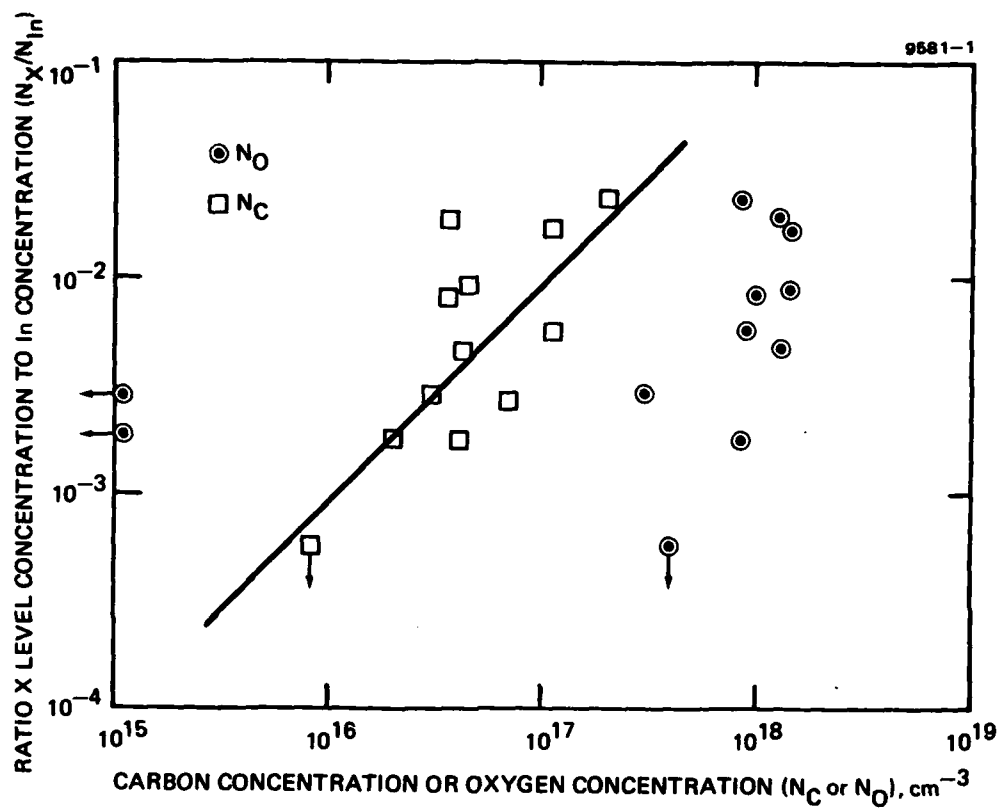


Figure 1. The ratio of X-level concentration to In concentration versus the O and C concentrations.

development of calibration standards. Initial studies used an IR-measured sample as the calibrating standard, while more recent work is using graphite and oxidized aluminum.

The results obtained at this stage of the study are listed in Table 3. The agreement is extremely good in most cases, well within the confidence limits of the IR measurements. The generally higher CPAA results obtained for the lower O and C concentrations and for the polycrystalline sample may in fact be real, since the IR method measures only those O and C atoms in their respective interstitial and substitutional positions. The CPAA method, on the other hand, measures the total O or C content. The very high concentration of C measured by CPAA in polycrystalline Si may reflect segregation of C at grain boundaries. The CPAA results indicate sensitivities for O of  $10^{14} \text{ cm}^{-3}$  and for C of  $10^{15} \text{ cm}^{-3}$ .

#### D. ION IMPLANTATION OF In AND C

An experiment was performed to produce controlled amounts of X in Hall-effect samples by ion implanting controlled doses of In and C. The implants were done in four steps for each impurity so as to give a flat carrier concentration profile to a depth of about  $0.25 \mu\text{m}$ . Implant concentrations of In ranged from  $3 \times 10^{15} \text{ cm}^{-3}$  to  $1 \times 10^{17} \text{ cm}^{-3}$ ; concentrations of C ranged from  $1 \times 10^{16} \text{ cm}^{-3}$  to  $1 \times 10^{18} \text{ cm}^{-3}$ . Permutations in the order of species and implant energies were performed. All implants were done into n-type wafers that had a P concentration of about  $2.5 \times 10^{12} \text{ cm}^{-3}$ .

Hall samples were fabricated and were heated to  $900^\circ\text{C}$  for 30 min to anneal the implant damage; then the temperature was reduced to  $650^\circ\text{C}$  and held there for 30 min to produce a high X-level concentrations. Hall-effect measurements were made as a function of temperature and the results analyzed to determine the In, X, and net donor concentrations.

The In concentrations thus obtained were in agreement with the values expected on the basis of the implant parameters. However, a large net donor concentration was observed in all cases. This value was in the range from  $5 \times 10^{15} \text{ cm}^{-3}$  to  $10 \times 10^{15} \text{ cm}^{-3}$ , which is several orders of

Table 3. Comparison of O and C in Si Determined by  
IR and CPAA

Sample	N <sub>O</sub> (IR)	N <sub>O</sub> (CPAA)	N <sub>C</sub> (IR)	N <sub>C</sub> (CPAA)
C74101UD	$9.7 \times 10^{17}$	(Standard)	$3.2 \times 10^{17}$	$3.5 \times 10^{17}$
C017IN (Poly)	$1.45 \times 10^{18}$	$1.37 \times 10^{18}$	$4.8 \times 10^{16}$	$1.6 \times 10^{19}$
C014IN	$1.3 \times 10^{18}$	$9.9 \times 10^{17}$		
C70401IN	$3.9 \times 10^{17}$	$4.0 \times 10^{17}$		
Z111UD	$<10^{15}$	$3.2 \times 10^{16}$		
Z008IN	$<10^{15}$	$7.9 \times 10^{15}$	$2.0 \times 10^{16}$	$2.2 \times 10^{16}$
Z7577UD	$<10^{15}$	$6.8 \times 10^{15}$	$<2 \times 10^{15}$	$4.7 \times 10^{15}$
C71601IN			$7.7 \times 10^{15}$	$9.0 \times 10^{15}$
All units are cm <sup>-3</sup>				

7024

magnitude higher than the residual P content of the wafers. This donor concentration was higher than the predicted X-level concentration and made its quantitative evaluation impossible.

The most likely cause of this high a net donor concentration is unannealed implantation damage. Further annealing to remove or reduce this damage is clearly indicated.

#### E. FZ AND Czo ANNEAL STUDIES

Samples from FZ refined and Czo crystals were given a sequence of anneals at various temperatures, and Hall-effect measurements versus temperature were made between each anneal. The purpose of this study was to determine the thermal equilibrium X-level concentration as a function of anneal temperature and to compare it with the relationship predicted by the mass-action law.

The anneal condition and the X-level and net donor concentrations are given in Tables 4 and 5 for samples from the FZ ingot Z008IN and Czo ingot C019IN, respectively. Six different samples from Z008IN were studied: Z2, M6, D1, D2, D3, and D4. The third digit in the sample designation indicates the anneal state. In the cases of Z2 and M6, 0 in this position indicates unannealed or as-grown material (these samples had only a 610°C heat treatment for a few minutes to alloy the evaporated Al contacts). The samples were then sequentially annealed as indicated by the increasing letter designation. Most of the samples received 1-hr anneals, and all were quenched after annealing. Thus, sample Z2 was first measured before anneal, annealed at 850°C for 1 hr, measured, annealed at 650°C for 1 hr, measured, etc. The samples designated D were separate samples from the same wafer and had the indicated anneals. The sample M came from the middle of the ingot and had higher In and X concentrations than samples Z and D, which came from nearer to the seed end of the crystal. The Czo sample M3 had an anneal sequence analogous to sample Z2. Sample M3B was a rerun of M3A two years later with no intervening high-temperature anneal.

Table 4. Anneal Sequence Results for Ingot Z008IN

Sample Designation	Anneal Temperature, °C	$N_X$ , $10^{14} \text{ cm}^{-3}$	$N_D - N_B$ , $10^{14} \text{ cm}^{-3}$
Z20	As grown	2.39	0.120
Z2A	850	0.405, 7.13	0.384, 0.356
Z2B	650	2.26	0.109
Z2C	850	0.34, 5.21	0.230, 0.289
Z2D	750	2.57	0.137
Z2E	700	1.96	0.109
Z2F	650	2.25	0.112
Z2G	600	1.95	0.105
Z2H	550/2 hr	1.84	0.098
Z2I	1000	3.74	2.25
Z2J	1000	5.12	3.42
M60	As grown	7.47	0.160
M6A	450/72 hr	No change	No change
M6B	650/30 min	No change	No change
M6C	850/15 min	8.67	0.202
M6D	900/3 hr	6.31	0.359
M6E	1000	1.58	1.49
D10	1000	3.04	3.14
D20	500	2.40	0.119
D30	650/30 min	2.27	0.121
D40	850	0.354, 5.74	0.336, 0.305
All anneals are for 1 hr unless otherwise indicated.			

Table 5. Anneal Sequence Results for Ingot C019IN

Sample Designation	Anneal Temperature, °C	$N_X$ , $10^{14} \text{ cm}^{-3}$	$N_D - N_B$ , $10^{14} \text{ cm}^{-3}$
M3O	650/30 min	19.5	1.94
M3A	850	2.15, 44.4	2.06, 2.02
M3B	Retake data	2.13, 48.3	2.05, 2.04
M3C	800	1.15, 14.4	1.05, 0.774
M3D	750	12.0	0.650
M3E	700	13.3	0.812
M3F	650	20.1	1.64
M3G	600	24.5	2.79
M3H	600	28.9	3.65
M3I	550/2 hr	13.0	13.2
M3J	550	14.9	15.3
M3K	500	15.7	16.2
M3L	500/3 hr	Not detected	172
M3M	850	3.94	4.45
All anneals are for 1 hr unless otherwise indicated.			

7024

Two sets of results are presented for the anneal temperatures around 850°C. The analysis of the Hall-effect data involves the minimization of the sum of the squares of the errors between the data and the value predicted by the model at each temperature. Since the equations generated by the model are nonlinear in the parameters, an iterative approach is taken using several sets of randomly chosen initial parameters. Generally, the various sets either diverge or all converge to one solution. However, in the case of Si:In annealed near 850°C, two or more solutions often emerge from this procedure. The principal difference is in the X-level concentration and energy level obtained.

Thus, two sets of values are given for the anneal temperatures in this range. The explanation of this effect continues to elude us and there is no way to determine, a priori, which solution is correct. To resolve this dilemma, a spectral photoconductive measurement was made on the sample from C019IN. No X level was observed. Since our limit of detectability was  $1 \times 10^{15} \text{ cm}^{-3}$ , it can be concluded that the lower X-level value is correct.

These results are plotted versus the reciprocal of the anneal temperature in Figures 2 and 3 for crystals Z008IN and C019IN, respectively. Several trends can be seen in the data. The donor concentration of the Czo samples increases with decreasing anneal temperature at the lower temperatures, while the FZ samples do not show this effect. This increase has been determined to result from the formation of oxygen donors.<sup>7</sup> The donor concentration tends to increase at the highest anneal temperatures for both the Czo and FZ crystals. This unexpected result has not been explained. Oxygen-donor complexes must be ruled out as the cause since this effect is seen in the FZ crystal, which did not exhibit the low-temperature oxygen-related behavior.

An attempt was made to getter possible defect complexes in sample Z008IN.22J. A heavy dose of phosphorus was implanted into the back of this sample so as to create considerable lattice damage. The sample was then annealed for an additional hour at 1000°C, after which the damaged

implanted layer was removed by etching. The subsequent Hall analysis showed that both donor and X concentrations went up. Thus, either no gettering took place (which is unlikely) or the increase in donors is not defect related. It was also observed that the surface morphology of the sample after the etch was extremely bad.

The most striking result of this anneal study, as revealed in Figures 2 and 3, is that the X-level concentration in the FZ samples is anneal independent! The Czo sample exhibits the inverse temperature relationship that is predicted by the mass-action law, but the FZ samples appear to be in violation. Thus, whatever the X-level model, there clearly is a significant difference between FZ and Czo samples in the way they respond to heat treatment. We believe that this fact has serious implications for the processing of high-speed large-scale-integration (LSI) devices.

In the present case, we believe that the FZ data result from the In-C pairs not reaching their thermal equilibrium distribution. Extrapolation of In and C diffusion data indicate that thermal equilibrium of In-C pairs should not be obtained in this material. We believe that the diffusion of C in Czo material is greatly enhanced, perhaps by the presence of O.

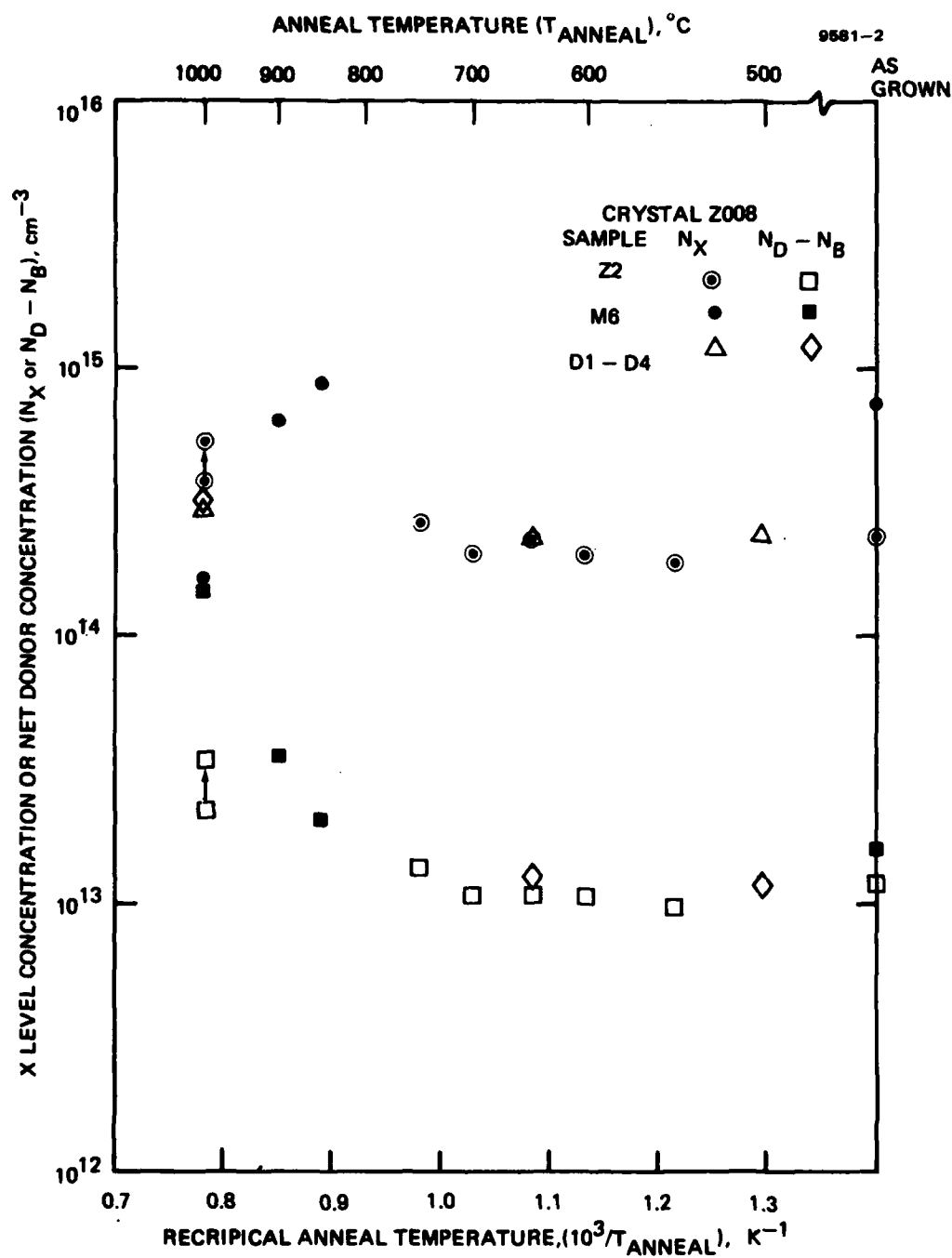


Figure 2. X-level and donor concentrations as functions of anneal temperature for crystal 2008.

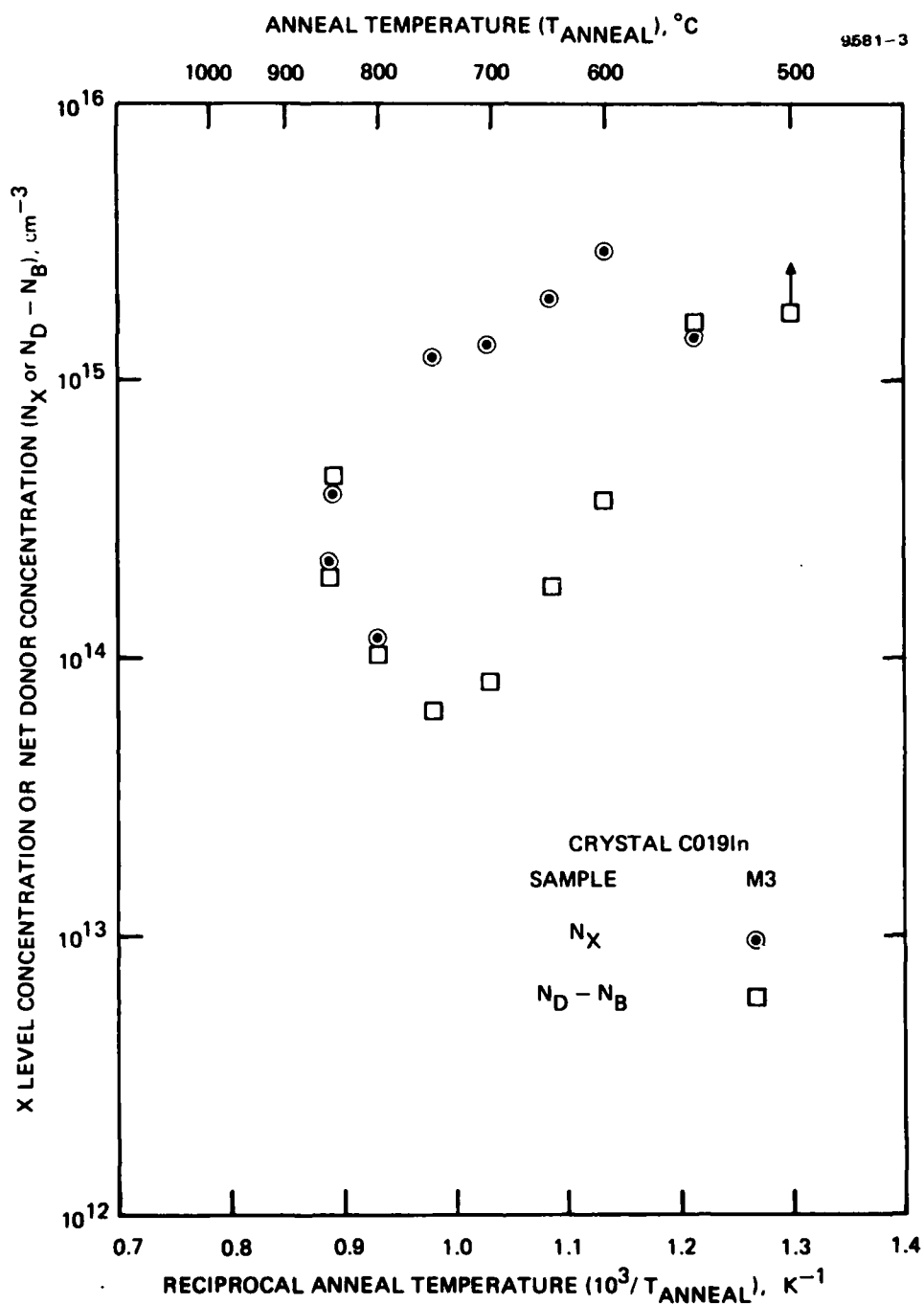


Figure 3. X-level and donor concentrations as functions of anneal temperature for crystal C019.

### SECTION 3

#### PHOTOLUMINESCENCE STUDIES IN EXTRINSIC SILICON

This section, which describes work done at CIT during this reporting period, was written by Professor T.C. McGill.

The primary aim of this program has been to develop photoluminescence as a technique for exploring the properties of Si doped for detector application with particular emphasis on Si:In.

The photoluminescence experiments have been aimed at giving a detailed explanation of the very rich photoluminescence spectra observed for indium-doped Si samples (Si:In). A typical spectrum is given in Figure 4. We have been attempting to identify the various previously unidentified lines and to study their variation from sample to sample. Detailed studies of the lines labeled P, Q, R, and  $U_1$  in Figure 4 have been carried out. These lines are of interest since they are observed only in the Si:In samples and may be due to various defects in these samples. These lines, with the exception of the  $U_1$  line, show rather large variations from sample to sample as shown in Figure 5. During the period covered by this report, we have completed our studies of the lines labeled P, Q, R, and  $U_1$ . These studies have allowed us to make identifications of these lines.

We are continuing to investigate the spectral region where we would expect to see the X level. However, this spectral range contains a number of weak lines from the argon ion laser and we are having to sort out these lines from lines due to the X level.

##### A. OBSERVATION OF LONG LIVED LINES IN Si:In, THE P, Q AND R LINES

We have made a detailed study of the P, Q, and R lines because they are rather intense and observed only in Si:In samples. One of the most striking features of these lines is their very long lifetime:  $\sim 200$   $\mu$ sec. This value should be compared to that for the In-bound exciton line at about 3 nsec and the boron-bound exciton at 1  $\mu$ sec. This very long lifetime indicates that the lines are due to an isoelectronic

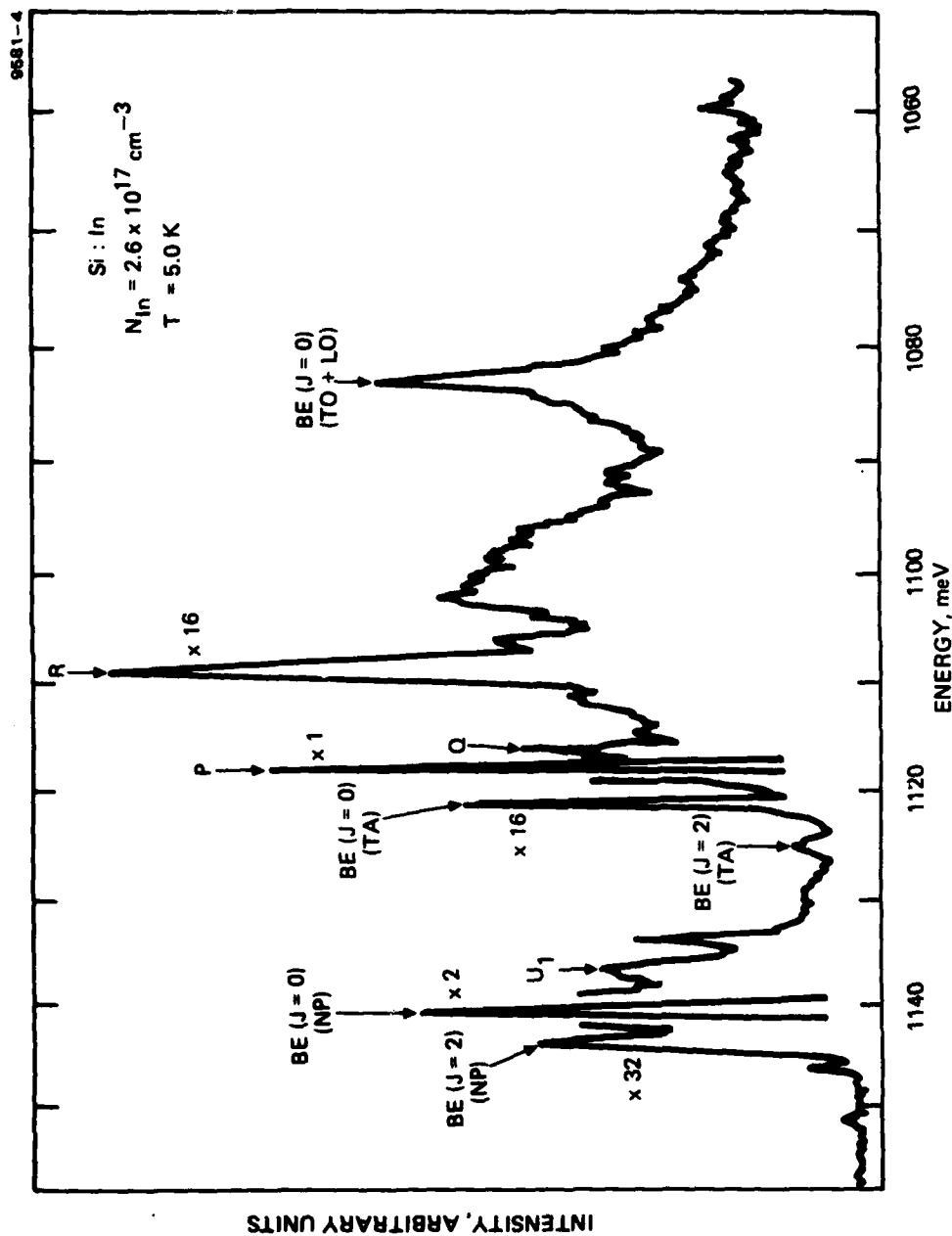


Figure 4. A representative photoluminescence spectrum for indium-doped Si. The lines labeled BE are due to an exciton bound to a neutral indium atom. The P, Q, R, and  $U_1$  lines are discussed in the text.

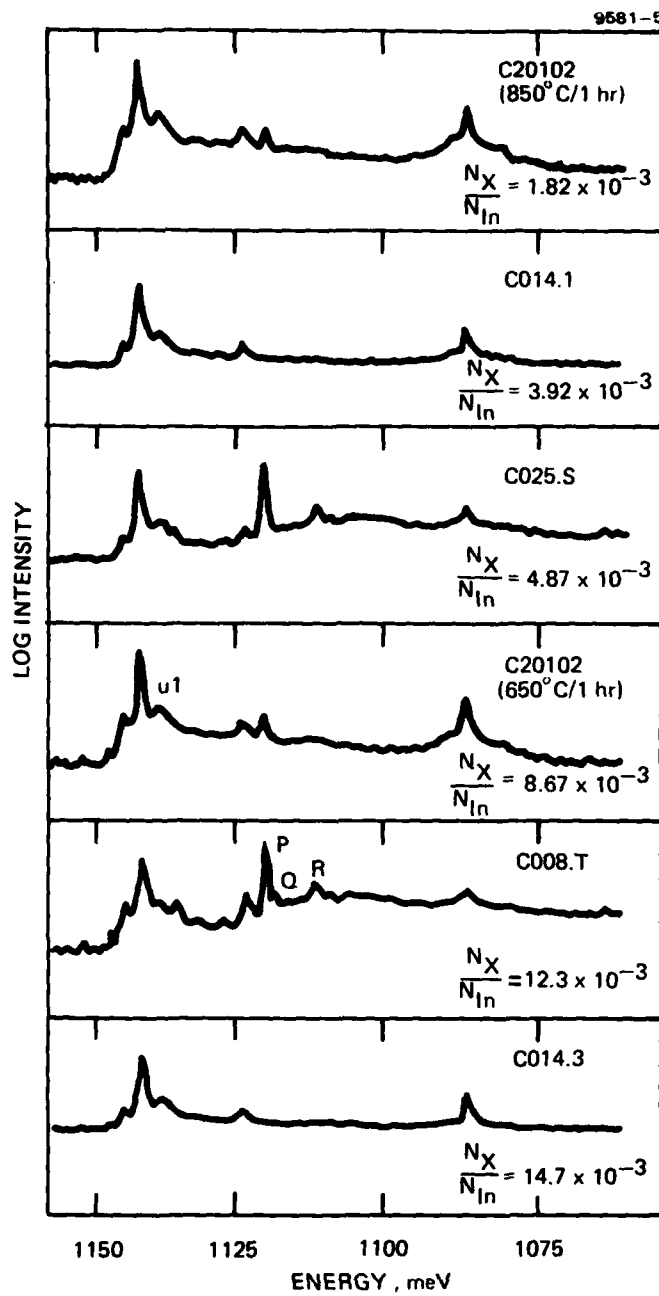


Figure 5. The photoluminescence spectra from several Czochralski-grown, indium-doped Si samples. The positions of the P, Q, R, and  $U_1$  lines are shown.

center (perhaps a donor-acceptor pair) and that the radiative efficiency should be nearly one. Hence, while the lines are rather intense ( $I_p/I_{In_{Be}} \sim 1$ ), the density of centers producing these lines may be five orders of magnitude less dense than the density of In. Since these lines seem to come from an isoelectronic center, it seems likely that they would not show up as electrically active centers in the Si:In material.

A detailed account of this work has been published in Solid State Communications.<sup>8</sup> The manuscript is included as Appendix B.

#### B. EVIDENCE FOR JAHN-TELLER SPLITTING OF THE GROUND STATE OF Si:In

The  $U_1$  line occurs at slightly lower energies than the line due to the bound exciton. This line was initially thought to be due to a multi-exciton complex on the Si:In center. However, more recent investigations of the dependence of the  $U_1$  line on pump power, temperature, and doping show that the ratio of the intensity of this line,  $I_{U_1}$ , to that of the indium-bound exciton,  $I_{BE}$ , is independent of all these parameters. This observation indicates that the  $U_1$  line is the result of a transition to an excited state of the neutral indium acceptor about 4.1 meV above the ground state.

Such an excited state of the In acceptor is to be accepted based on simple Jahn-Teller considerations. As illustrated in Figure 6, the ground state of the indium acceptor can be split by moving the indium atom off the substitutional site. One of the levels goes down to lower energy while one goes to higher energy. This distortion results in two levels split by an energy  $\Delta E$ . Ultrasonic absorption experiments<sup>9</sup> on Si:In have suggested that this distortion does occur and that the splitting is about 4.1 meV.

A more detailed report on this work was published in Physics Letters<sup>10</sup> and is included as Appendix C.

9581-6

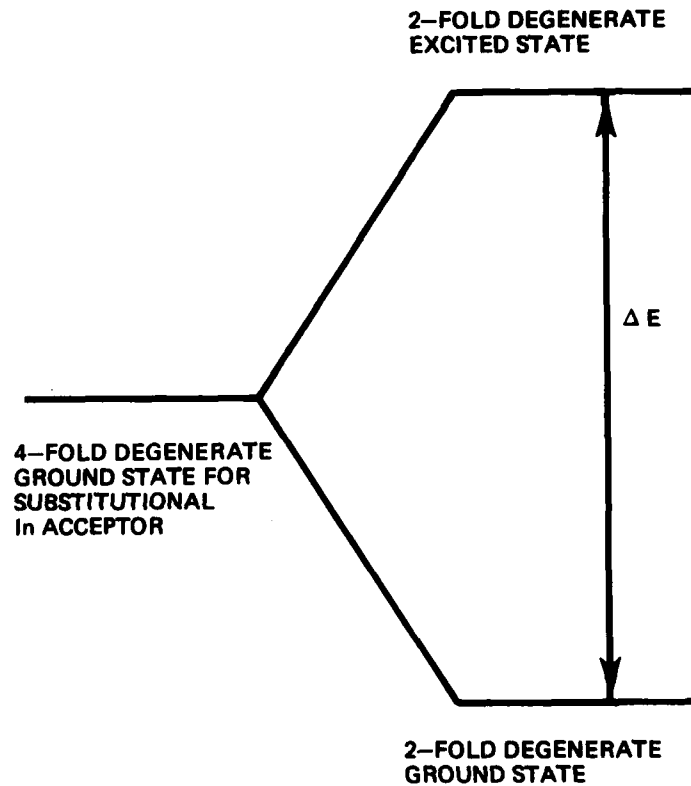


Figure 6. A schematic of the energy levels on a neutral indium. The levels to the left are for an indium located in a substitutional site. Those on the right are for an In that is slightly off center.

### C. SEARCH FOR PHOTOLUMINESCENCE FROM THE X LEVEL

We can use Haynes rules as a guide to the approximate energy for the photoluminescence from the X level.<sup>11</sup> This empirical rule states that the binding energy of the exciton is approximately a fixed fraction of the ionization energy of the neutral acceptor ( $E_A$ ) or donor ( $E_D$ ). If  $E_{FE}$  is the energy position of the threshold for free exciton emission, then the position of the X level is

$$E_{BE(A)} = E_{FE} - aE_A ,$$

where  $a$  is approximately 0.1. Fitting the known values of  $E_{BE(A)}$  for BE lines for  $A = B, Al, Ga,$  and  $In$  to this form gives a value for  $a$  of 0.09. This value of  $a$  combined with the binding energy for the X level, 111 meV,<sup>1</sup> and the free exciton threshold in the no-phonon transition gives a value of  $E_{BE(X)} \approx 1145$  meV. Examination of Figure 4 shows that there is a weak line in this spectral region. However, this line has been found to be due to the argon ion laser. We are presently exploring this spectral region with more care using excitation from a GaAs laser and a filtered Ar ion laser.

### D. EXCITATION TRANSFER

#### 1. Introduction

One of the major objectives of this program was the detection of background impurities and defects at concentrations substantially below that of the majority dopant (e.g., "X" level" in Si:In).<sup>1</sup> This objective required the ability to detect luminescence from excitons bound to one center in the presence of large concentrations of a second center. Although photoluminescence has been successfully used to detect concentrations of boron and phosphorus in Si at low impurity concentrations,<sup>12</sup> the technique has not been applied to the cases of interest here.

As the investigation developed, it was observed that, in some cases, the luminescence from background impurities was anomalously small. Hence, we initiated a careful study of the photoluminescence intensities of B and In in Si as a function of B and In concentrations ( $N_B$  and  $N_{In}$ , respectively). Si:(B,In) was chosen as a model system for the study for the following reasons. First, both B and In bound exciton (BE) luminescence have been studied extensively and the spectra are well characterized.<sup>13,14</sup> Also, the decay mechanisms for excitons on B and In have been identified<sup>15</sup> and the decay rates have been measured.<sup>16,17</sup> Finally, the capture cross section for excitons on In<sup>18,19</sup> and B<sup>10,20</sup> have been determined as a function of temperature.

The results of this study suggest that it is not possible to use photoluminescence to detect background impurities in the presence of large concentrations of a majority dopant.

## 2. Rate Theory of Photoluminescence Spectra

The model system chosen for this investigation is governed by a simple set of rate equations. If we let:

- $g$  = the generation rate of free excitons
- $n_{FE}$  = the density of free excitons
- $\tau_{FE}$  = the direct decay time for free excitons
- $\sigma_B$  = the capture cross section for excitons on B
- $\sigma_{In}$  = the capture cross section for excitons on In
- $N_B$  = the density of B in the sample
- $N_{In}$  = the density of In in the sample
- $N_{FE}$  = the thermally averaged free exciton density of states
- $n_B$  = the density of B atoms with excitons bound to them
- $n_{In}$  = the density of In atoms with excitons bound to them

$E_B$  = the binding energy of an exciton bound to a B

$E_{In}$  = the binding energy of an exciton bound to an In

$\tau_B$  = the lifetime of a B bound exciton

$\tau_{In}$  = the lifetime of an In bound exciton

$v_{th}$  = the thermal velocity of excitons,

then we have

$$\begin{aligned} \frac{dn_{FE}}{dt} = & g - \frac{n_{FE}}{\tau_{FE}} - \sigma_B v_{th} (N_B - n_B) n_{FE} \\ & + N_{FE} \sigma_B v_{th} n_B e^{-E_B/kT} - \sigma_{In} v_{th} (N_{In} - n_{In}) n_{FE} \\ & + N_{FE} \sigma_{In} v_{th} n_{In} e^{-E_{In}/kT} \end{aligned} \quad (1)$$

$$\frac{dn_B}{dt} = \sigma_B v_{th} (N_B - n_B) n_{FE} - N_{FE} \sigma_B v_{th} n_B e^{-E_B/kT} - \frac{n_B}{\tau_B} \quad (2)$$

$$\begin{aligned} \frac{dn_{In}}{dt} = & \sigma_{In} v_{th} (N_{In} - n_{In}) n_{FE} - N_{FE} \sigma_{In} v_{th} n_{In} e^{-E_{In}/kT} \\ & - \frac{n_{In}}{\tau_{In}} \end{aligned} \quad (3)$$

These equations can be solved quite simply for a steady-state solution if we assume:

- (i) temperatures sufficiently low that we can neglect the thermal release terms, and
- (ii) pump powers sufficiently low that we can assume  $n_B \ll N_B$  and  $n_{In} \ll N_{In}$ .

In this limit, we obtain the equations

$$n_{FE} = \frac{g}{(N_B \sigma_B + N_{In} \sigma_{In}) v_{th}} \quad (4)$$

$$n_B = N_B \sigma_B v_{th} \tau_B n_{FE} = \frac{N_B \sigma_B \tau_B g}{N_B \sigma_B + N_{In} \sigma_{In}} \quad (5)$$

$$n_{In} = N_{In} \sigma_{In} v_{th} \tau_{In} n_{FE} = \frac{N_{In} \sigma_{In} \tau_{In} g}{N_B \sigma_B + N_{In} \sigma_{In}} \quad (6)$$

From these equations, we obtain the expression

$$\frac{I_B}{I_{In}} = R \frac{N_B}{N_{In}}, \quad (7)$$

where

$$R \equiv \frac{f_B \sigma_B \tau_B}{f_{In} \sigma_{In} \tau_{In}} \quad (8)$$

and

$I_B$  = B bound exciton luminescence intensity,

$I_{In}$  = In bound exciton luminescence intensity,

$f_B$  = B bound exciton oscillator strength,

$f_{In}$  = In bound exciton oscillator strength.

This result indicates how we had planned to measure concentrations of various defects and impurities in the Si:(B,In) model system. Since the ratio R is independent of pump power and concentration, a single calibration of the factor R would allow us to obtain the value of  $N_B$

from a knowledge of  $R$ , the ratio of the BE luminescence intensities, and  $N_{In}$ . The relationship is:

$$N_B = \frac{1}{R} N_{In} \left( \frac{I_B}{I_{In}} \right) . \quad (9)$$

However, Eqs. 4-6 describe an additional feature of the model system not contained in Eq. 9. Consider the situation in which  $N_{In}$  is increased while the generation rate  $g$  (that is, the laser pump power) and  $N_B$  are held constant. As Eq. 4 indicates, this results in a decrease in the free exciton density,  $n_{FE}$ . According to Eq. 5, a decrease in  $n_{FE}$  in turn results in a decrease in the B bound exciton density,  $n_B$ . Since the B bound exciton luminescence intensity,  $I_B$ , is proportional to  $n_B$ , the final result is a decrease in  $I_B$ .

As a result of this coupling of  $N_{In}$  and  $I_B$  through the free exciton gas, the rate theory of the model system predicts that it may be possible to completely quench the B bound exciton luminescence simply by increasing the concentration of In dopant.

Of course, increasing the laser pump power increases  $g$  and therefore  $n_{FE}$ . So it may be possible to some extent to overcome the effect described above by increasing the pump power. However, at higher pump powers, sample heating can become an important factor. Then the thermal release terms in the rate equations for the model system become important, and Eq. 9 is no longer justified. Although it is possible to include the thermal release terms in the analysis, the sample heating effect is one which is difficult to quantify. For routine analysis, it becomes exceedingly desirable to operate in a pump power region in which sample heating effects are negligible.

### 3. Experimental Results

To systematically investigate the applicability of the rate theory, we have measured the pump power dependence of the intensity of the B and In BE lines and the dependence of R on the values of  $N_B$  and  $N_{In}$ . All the samples studied and the concentrations as measured by Hall effect are given in Table 6.

#### a. Pump Power Dependence

This initial investigation was designed to determine the experimental conditions under which Eqs. 4 through 6 and therefore Eq. 9 are justified. Eqs. 5 and 6 predict that  $I_B$  and  $I_{In}$  vary linearly with pump power, and these measurements demonstrate the range of pump powers for which this is the case.

The pump power dependence of the transverse optical phonon replica of the B bound exciton luminescence line ( $B_{TO}$ ) for sample Z104011 is shown in Figure 7. As this figure demonstrates, the intensity varies linearly with the pump power for pump powers ranging from 0.1 to 1.0 mW and varies sublinearly for pump powers greater than 10 mW. While it is difficult for us to get a precise measure of the spot size for our exciting laser, it is approximately 4 mm in diameter. The deviation in the point at 10 mW from the linear relation observed at lower powers is due to saturation of the B centers with excitons.

Similar results have been obtained for the In line. The data for the intensity of the no-phonon replica ( $I^{NP}$ ) is presented in Figure 8. In this case, the intensity is linear over the entire range of pump powers. It is much more difficult to saturate the In line in these samples because of the higher concentration of In centers and the short lifetime of the In bound exciton ( $\tau_{In} \cong 3 \text{ nsec}^{17}$  as compared to  $\tau_B \cong 1.0 \text{ } \mu\text{sec}^{16}$ ).

Measurements similar to these were carried out for each sample studied. Care was then taken to ensure that subsequent measurements were made under conditions for which Eqs. 4 through 6 were justified.

Table 6. Si:In:B Photoluminescence Samples

Sample	$N_B$ , $\text{cm}^{-3}$	$N_{In}$ , $\text{cm}^{-3}$	$N_B/N_{In}$
Z20601	$5.2 \times 10^{12}$	$1.0 \times 10^{17}$	$5.2 \times 10^{-5}$
C11204.T	$1.4 \times 10^{14}$	$1.3 \times 10^{17}$	$1.1 \times 10^{-3}$
C11204.M	$0.63 \rightarrow 1.4 \times 10^{14}$	$3.4 \times 10^{16}$	$1.8 \rightarrow 4.1 \times 10^{-3}$
C11204.S	$6.3 \times 10^{13}$	$1.3 \times 10^{16}$	$4.8 \times 10^{-3}$
Z20601R	$9.8 \times 10^{13}$	$3.6 \rightarrow 5.1 \times 10^{16}$	$1.9 \rightarrow 2.7 \times 10^{-3}$
Z074	$3.9 \times 10^{13}$	$1.7 \times 10^{16}$	$2.3 \times 10^{-3}$
C117.S	$7.8 \times 10^{13}$	$2.1 \times 10^{16}$	$3.7 \times 10^{-3}$
C112.M	$4.25 \times 10^{15}$	$2.4 \times 10^{17}$	$1.8 \times 10^{-2}$
Z20601A	$1.9 \times 10^{14}$	$5.5 \times 10^{15}$	$3.5 \times 10^{-2}$
Z104011	$2.7 \times 10^{13}$	$2.0 \times 10^{14}$	0.135
Z163.T	$3.9 \times 10^{13}$	$2.2 \times 10^{13}$	1.77
Z163.S	$3.5 \times 10^{13}$	$6.8 \times 10^{12}$	5.15
The numbers identifying the samples correspond to the ingot number at HRL. All the concentrations were determined from Hall-effect versus temperature measurements made at HRL.			

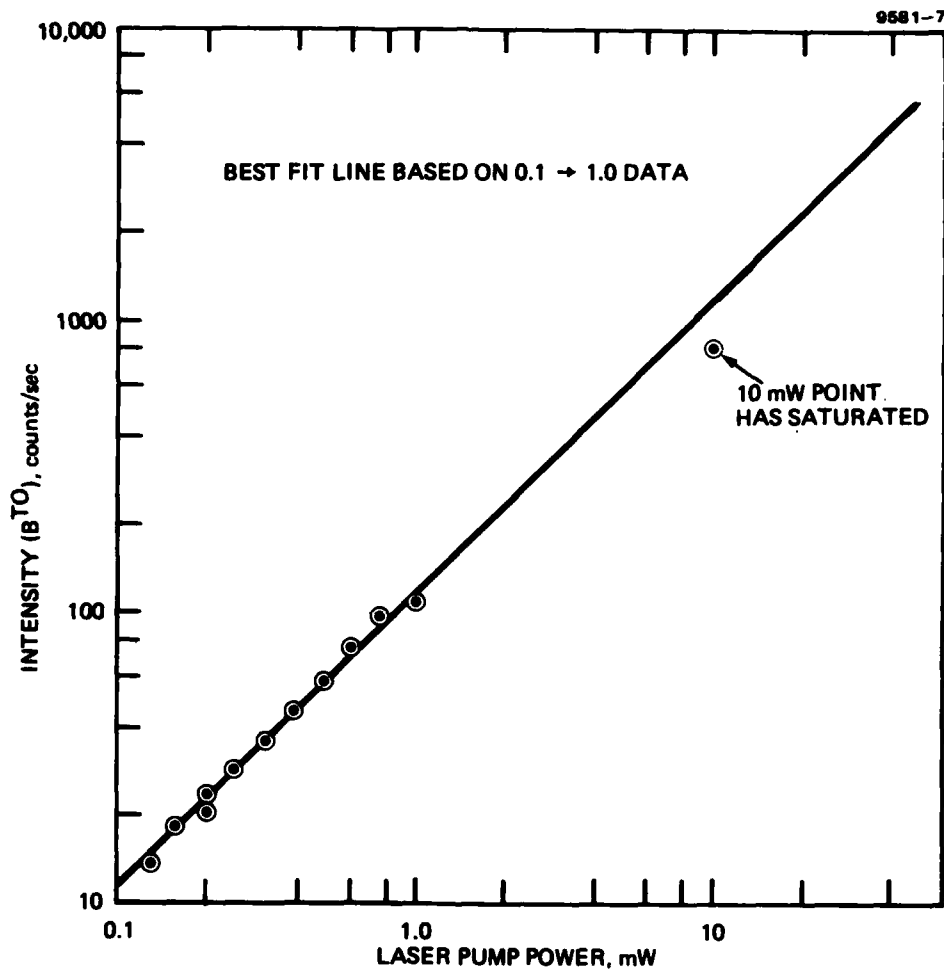


Figure 7. The intensity of the bound exciton (BE) due to boron in the T<sub>0</sub>-phonon replica as a function of pump power. The data is for sample Z104011 as described in Table 6.

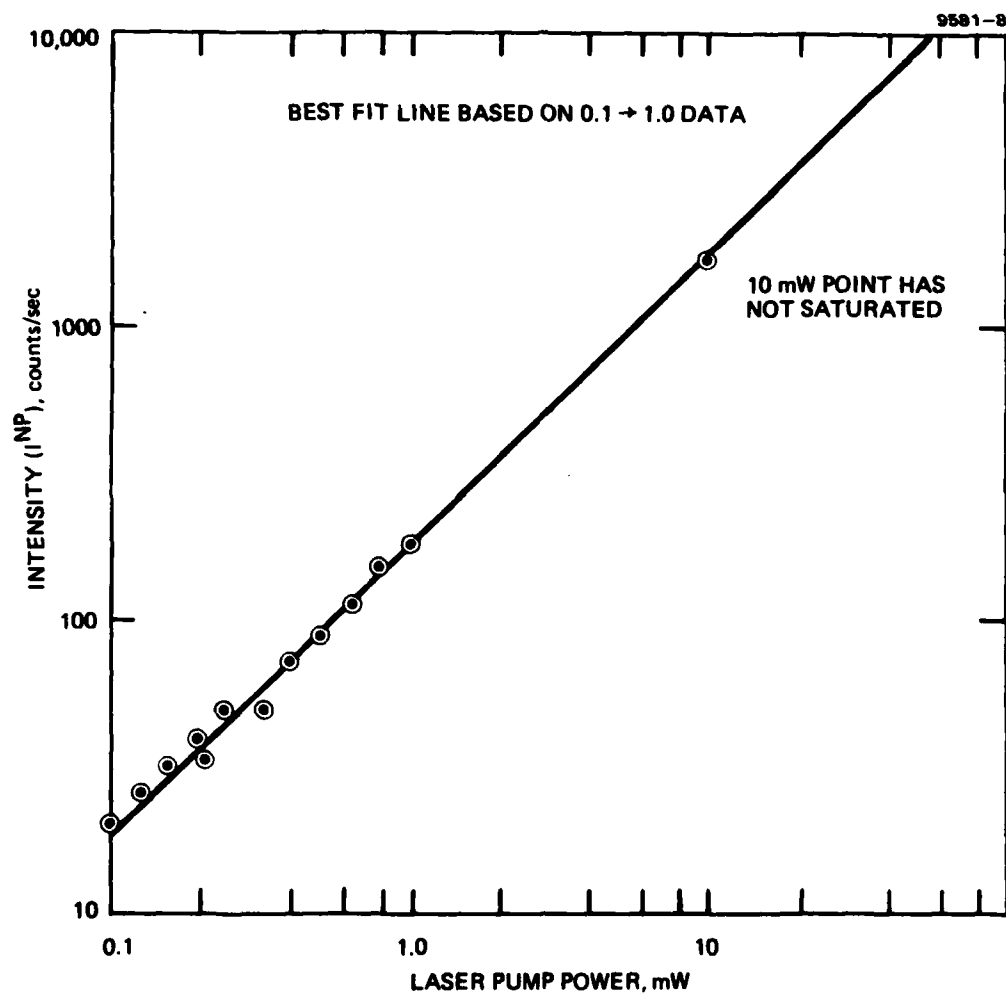


Figure 8. The intensity of the bound exciton (BE) due to indium in the no-phonon replica as a function of pump power. The data is for sample Z104011 as described in Table 6.

b. Variation of R with  $N_{In}$  and  $N_B$

The most important prediction of the theory that must be verified is the independence of R from  $N_{In}$  and  $N_B$ . We have made measurements of R for all the samples given in Table 6. The results are summarized in Figure 9, which is a plot of R versus  $N_{In}$ . As can be seen from Figure 9, within experimental error, R is independent of  $N_{In}$  for  $N_{In}$  between  $6 \times 10^{12} \text{ cm}^{-3}$  and about  $10^{15} \text{ cm}^{-3}$ . The value of  $N_B$  for each of the samples is given in Table 6.

For  $N_{In} > 5 \times 10^{16} \text{ cm}^{-3}$  (samples Z20601, Z20601R, Z074, C117, C11204.T, C11204.M, C11204.S, and C112.M) the boron BE line could not be observed and, hence, no point is plotted on Figure 9. With the exception of sample C112.M, the inability to see B in luminescence could be attributed to the quenching of  $I_B$  by high In dopant concentrations, as predicted by Eqs. 4 through 6. For example, samples Z20601A and C11204.T have essentially the same B concentration. Naively, for a given pump power, one might expect to see the same B bound exciton luminescence intensity for these two samples. But sample C11204.T has about 60 times more In than sample Z20601A, which quenches the B bound exciton luminescence by reducing the free exciton density.

As discussed above, an increase in the pump power should compensate for this effect, until sample heating becomes important. To test this prediction, the luminescence from sample C11204.S was examined at higher pump powers. Sample C11204.S was chosen because it had the lowest In concentration of all the samples from which the B bound exciton luminescence was not visible. On the basis of the theory, then, sample C11204.S should require the smallest pump power increase to overcome the quenching effect of high In concentration. In fact, comparison of the B and In concentrations for samples C11204.S and Z20601A (from which the B bound exciton luminescence is visible) indicates that it would be quite reasonable to expect to see B bound exciton luminescence from sample C11204.S at pump powers for which sample heating is not

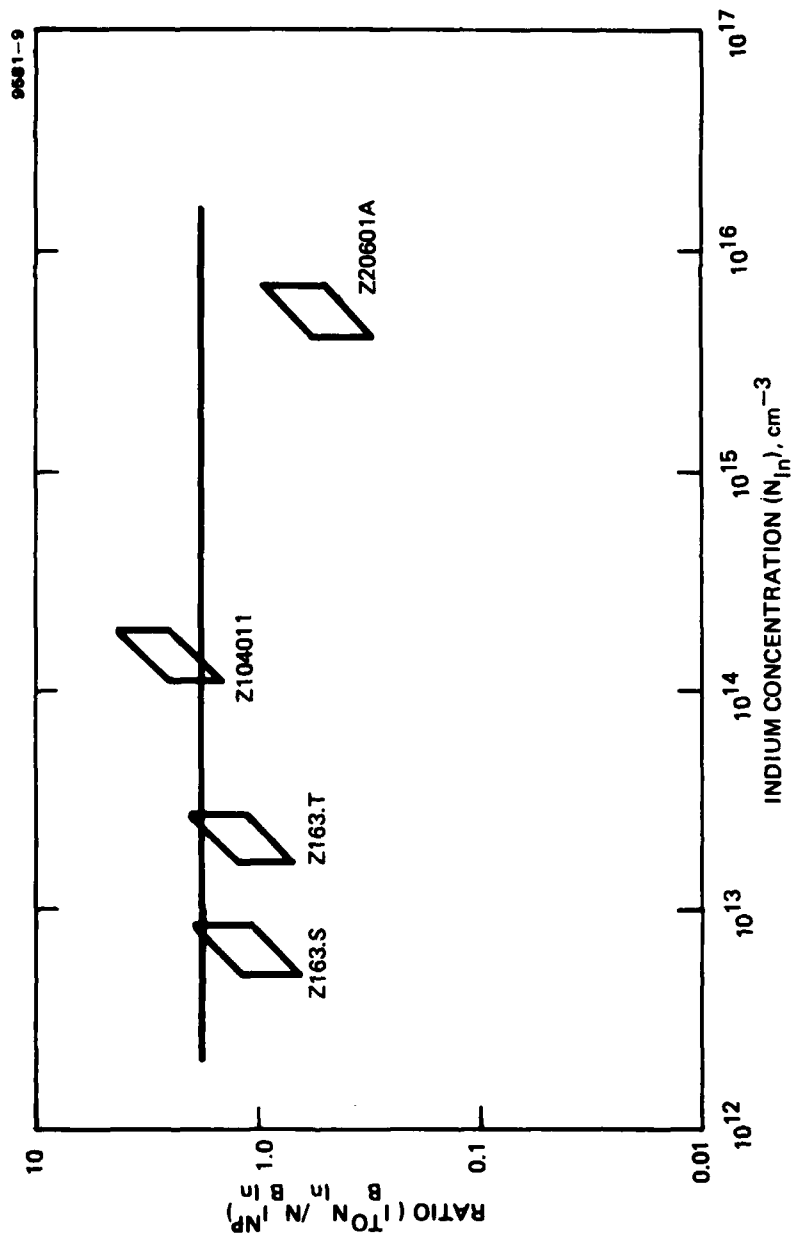


Figure 9. The ratio  $I_B^{TO} N_{In} / N_B I_{In}^{NP}$  as a function of  $N_{In}$ . The parameters for the various samples are given in Table 6. The error bars are based on estimates of the errors in  $N_B$ ,  $N_{In}$ ,  $I_B^{TO}$ , and  $I_{In}^{NP}$ .

important. The luminescence from sample C11204.S was examined at various pump powers up to 2 W. No B bound exciton luminescence was observed.

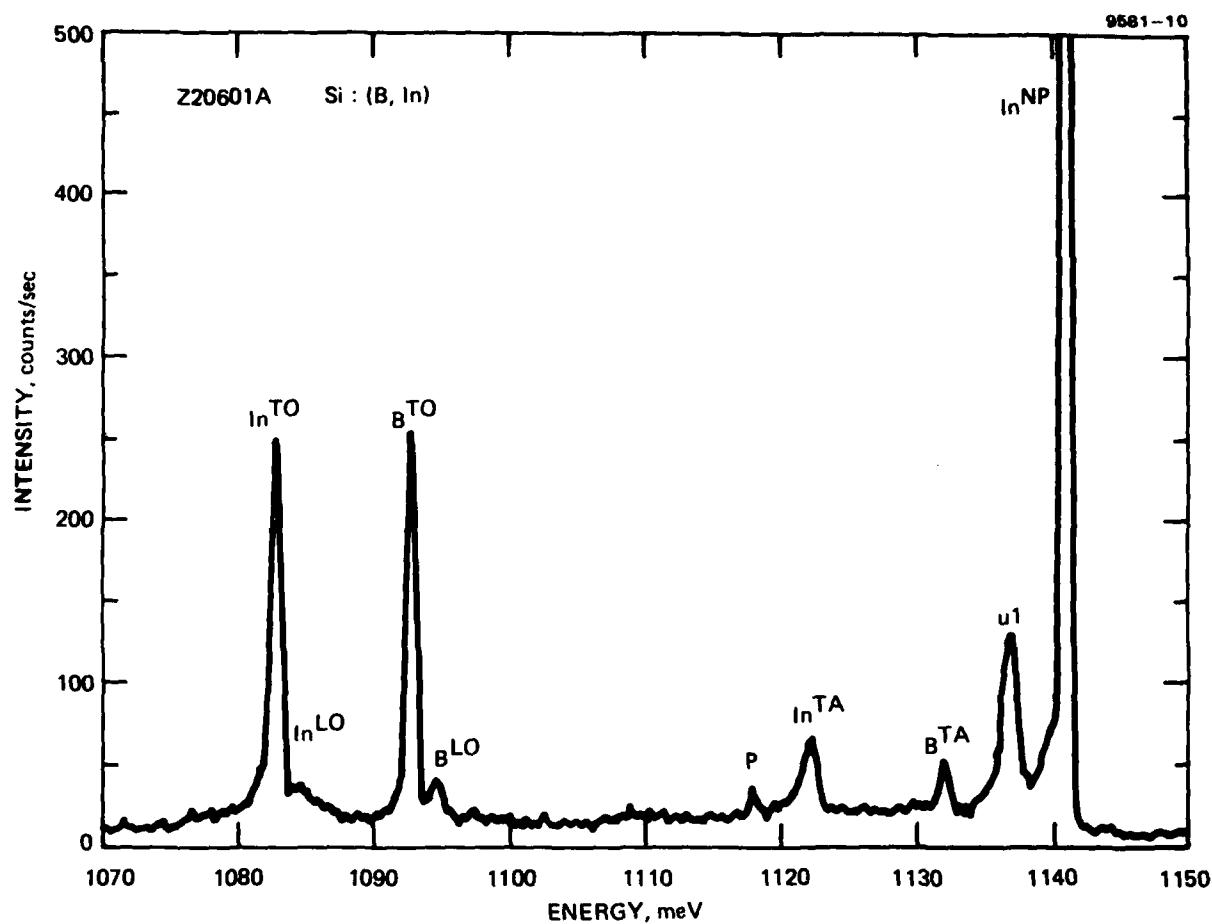
This result is an indication that the theory presented above becomes inapplicable at high concentrations. Examination of sample C112.M provides further evidence. For example, compare sample C112.M with sample Z20601A. While it is true that sample C112.M has about 40 times more In than sample Z20601A, the ratio  $N_B/N_{In}$  has remained virtually constant. On the basis of our theory, we would have expected  $I_B/I_{In}$  to have remained constant as well. Examination of Figure 10 reveals that this is not the case.

We have plotted the spectra from samples C112.M and Z20601A in Figure 10(a) and (b), respectively. In the spectrum from sample Z20601A, we see the intense BE lines due to In labeled  $In^{NP,TA,TO,LO}$  and the lines due to B labeled  $B^{TA,TO,LO}$ . We also see the  $U_1^{10}$  and  $P^8$  lines which we have previously observed. In the spectrum for C112.M, the intense In lines are still present. However, the boron lines are absent. Using the ratio obtained from the previous experiments, we would expect  $I_B^{TO}$  to be about 80 counts/sec. It is simply not visible.

This result actually proves that, at high In dopant concentrations, the rate theory presented above breaks down. R is no longer independent of  $N_B$  and  $N_{In}$ . The last point plotted in Figure 9, for sample Z20601A, may indicate the threshold for this effect, since it is well below the "constant R" line established for lower values of  $N_{In}$ . However, more data in this region of  $N_{In}$  is needed before a threshold can be firmly established.

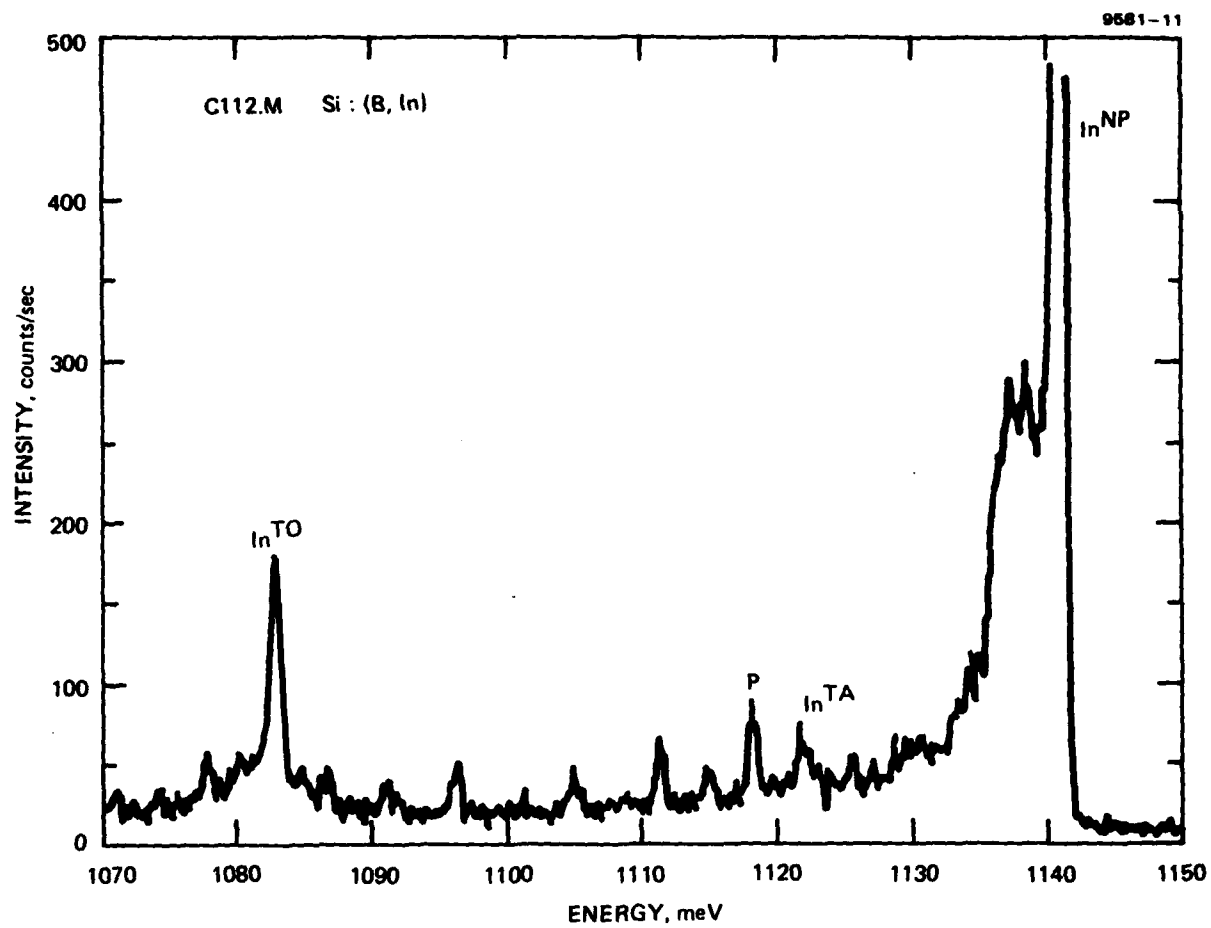
#### 4. Conclusions

The rate theory presented in Section 3.D.2 suggested that a measurement of the ratio of  $I_B$  to  $I_{In}$  would provide the relative concentrations of the two species. However, the experiments uncovered two pitfalls in this program:



a. Z20601A Si:(B,In)

Figure 10. The photoluminescence spectra of two samples: Z20601A and C112M. The various lines are discussed in the text.



b. C112.M Si: (B, In)

Figure 10. Continued.

1. The pump power must be kept low enough so that none of the centers of interest saturate, and so that the sample does not heat substantially. At these pump powers ( $\sim 1$  mW to 10 mW), quenching of background B bound exciton luminescence at In dopant concentrations of  $\sim 10^{16} \text{ cm}^{-3}$  was observed.
2. At high concentrations, the data shows that R is not independent of  $N_{\text{In}}$ . It is likely that this phenomenon occurs because of some exciton transfer process in which excitons hop from the B to the In. The precise nature of this process is still undetermined.

These results make it difficult to see how photoluminescence can be used to measure the concentration of a secondary impurity at low concentrations in the presence of another dopant at much higher concentrations. As a consequence, it will be difficult to use photoluminescence to study the "X level" in heavily doped Si:In, where the Hall-effect has clearly indicated the presence of this center.

### References

1. R. Baron, M.H. Young, J.K. Neeland, and O.J. Marsh, Appl. Phys. Lett. 30, 594 (1977).
2. R.N. Thomas, T.T. Braggins, H.M. Hobgood, and W.J. Takei, J. Appl. Phys. 49, 2811 (1978).
3. R.D. Larrabee, Semiconductor Characterization Techniques. Edited by P.A. Barnes and G.A. Rozgonyi (Electrochemical Society, Princeton, 1978), p. 71.
4. W. Scott, Appl. Phys. Lett. 32, 540 (1978).
5. R. Baron et al., Appl. Phys. Lett. 34, 257 (1979). (Appendix A of this report).
6. J. Baukus and T. McGill, Interim Technical Report 2, contract DAAK-77-C-0082 (Army Night Vision and Electro-Optics Laboratory, Fort Belvoir, VA.), 1978.
7. A. Kanamori, Appl. Phys. Lett. 34, 287, (1979).
8. G.S. Mitchard, S.A. Lyon, K.R. Elliott, and T.C. McGill, Solid State Comm. 29, 425 (1979). (Appendix B of this report)
9. Hp. Schad and K. Lassmann, Physics Letters 56A, 409 (1976).
10. K.R. Elliott, S.A. Lyon, D.L. Smith and T.C. McGill, Phys. Lett. 70A, 52 (1979). (Appendix C of this report).
11. J.R. Haynes, Phys. Rev. Lett. 4, 361 (1960).
12. M. Tajima, Appl. Phys. Lett. 32, 719 (1978).
13. See for example K. Kosai and M. Gershenson, Phys. Rev. B9, 723 (1974).
14. See for example S.A. Lyon, D.L. Smith and T.C. McGill, Phys. Rev. B17, 2620 (1978); K.R. Elliott, G.C. Osbourn, D.L. Smith and T.C. McGill, Phys. Rev. B17, 1808 (1978).
15. G.C. Osbourn and D.L. Smith, Phys. Rev. B16, 5426 (1977).
16. S.A. Lyon, G.C. Osbourn, D.L. Smith and T.C. McGill, Solid State Comm. 23, 425 (1978).
17. W. Schmid, Phys. Stat. Solidi 84(b), 529 (1977).

18. K.R. Elliott, D.L. Smith and T.C. McGill, Solid State Comm. 24, 461 (1977).
19. R.M. Feenstra and T.C. McGill, (to be published).
20. R.B. Hammond and R.N. Silver, Appl. Phys. Lett. 36, 68 (1980).

APPENDIX A

NATURE OF THE 0.111-eV ACCEPTOR LEVEL IN  
INDIUM-DOPED SILICON

# Nature of the 0.111-eV acceptor level in indium-doped silicon<sup>a)</sup>

R. Baron, J. P. Baukus, S. D. Allen,<sup>b)</sup> T. C. McGill,<sup>c)</sup> M. H. Young, H. Kimura, H. V. Winston, and O. J. Marsh

Hughes Research Laboratories, 3011 Malibu Canyon Road, Malibu, California 90265

(Received 23 October 1978; accepted for publication 5 December 1978)

Strong evidence is presented that the *X*-level defect, which produces a 0.111-eV acceptor level in Si:In, is a substitutional In-substitutional C (In-C<sub>s</sub>) pair. The concentration of this defect follows a mass-action law with the In and C concentrations, the association constant being  $(1.4 \pm 0.3) \times 10^{-19} \text{ cm}^3$  at 650°C. Reversible changes in the *X*-level concentration between anneal temperatures of 650 and 850°C are observed, and a pair binding energy of  $0.7 \pm 0.1 \text{ eV}$  is estimated. The electronic properties and temperature dependence of the concentration of this center are found to be those expected for a nearest-neighbor In-C<sub>s</sub> pair.

PACS numbers: 71.55.Fr, 72.40.+w, 72.20.My, 78.20.Ge

A new acceptor level (*X* level) in indium-doped silicon, located at 0.111 eV from the valence band, has been reported by us.<sup>1</sup> This defect, with a smaller ionization energy than In, is of interest because it significantly reduces the maximum temperature at which background-limited infrared detector performance can be obtained.<sup>1,2</sup> We have observed the *X* level<sup>1,3,4</sup> in the low-temperature slope of Hall measurements versus temperature and in the photoconductive spectrum of Si:In. Other workers have subsequently observed this level, not only in Hall measurements and in photoconductive spectra,<sup>5,6</sup> but also in its excited-state absorption spectrum.<sup>7</sup>

We reported<sup>1</sup> a strong correlation between the concentrations of the *X* level and In and tentatively attributed the level to an In complex with carbon or with a Si interstitial or vacancy, or to an In pair. We now present evidence that an In-C pair on adjacent substitutional sites is the defect causing this acceptor level.

Hall measurements versus temperature were made and analyzed to determine the densities of *X* ( $N_X$ ) and of donors ( $N_D$ ), as previously described.<sup>1</sup> A new procedure, however, was used to determine  $N_{In}$ . We had found that the large temperature dependence of the neglected Hall scattering factor<sup>8</sup> for  $T \gtrsim 100 \text{ K}$  distorted  $p(T)$  sufficiently to cause an overestimate by about a factor of 2 in  $N_{In}$ <sup>1,9</sup> for large values of  $N_{In}$ . For these large values our normal experimental limitation,  $T < 325 \text{ K}$ , precluded the appearance of the exhaustion region. By extending the Hall measurement to sufficiently high temperatures to observe the exhaustion region for a number of samples, we empirically determined<sup>10</sup> a relation between  $N_{In}$  and resistivity at 297 K, which was used to obtain the values of  $N_{In}$  reported here.

Substitutional carbon and interstitial oxygen concentrations were determined by measuring infrared absorption. The double beam difference method<sup>11</sup> was used to obtain the

absorption spectra of the samples at 77 K using as a reference a zone-refined undoped Si sample containing carbon and oxygen below the detection limits ( $2 \times 10^{15} \text{ C/cm}^3$  and  $1 \times 10^{15} \text{ O/cm}^3$ ). This method compensates for reflection losses and cancels lattice absorptions which interfere with both the C and O absorption peaks. The samples were 0.18 cm thick and the spectral resolution (FWHM) was  $0.75 \text{ cm}^{-1}$  at the oxygen absorption ( $1107 \text{ cm}^{-1}$ ) and  $3.06 \text{ cm}^{-1}$  at the carbon absorption ( $607 \text{ cm}^{-1}$ ). Several conflicting values of the calibration factors have been reported.<sup>12</sup> We have used the following relationships between the concentrations of carbon,  $N_C$ , and oxygen,  $N_O$ , and the absorption coefficients  $\alpha$  at 77 K:

$$N_O/\alpha(1107 \text{ cm}^{-1}) = 1.43 \times 10^{17} \text{ cm}^{-2},$$

$$N_C/\alpha(607 \text{ cm}^{-1}) = 3.1 \times 10^{16} \text{ cm}^{-2}.$$

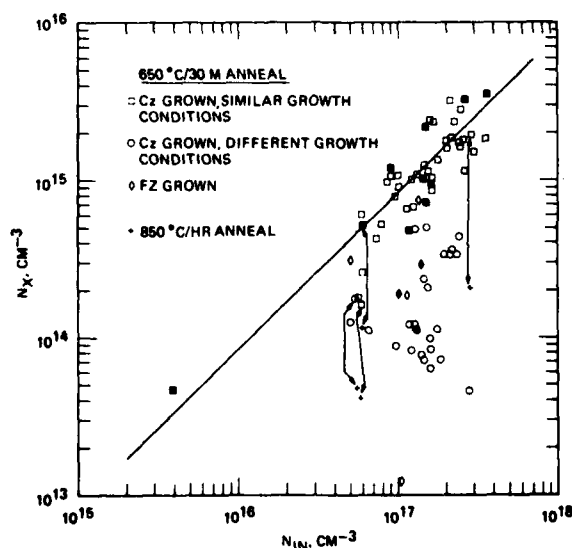


FIG. 1. *X*-level concentration versus indium concentration for Si:In crystals grown by a variety of methods. Arrows connect points for the same sample in different anneal states. Solid symbols are those displayed in Fig. 2. The line shown is a least-squares fit to the square symbols assuming unity slope.

<sup>a)</sup>Work was partially supported by the Defense Advanced Research Projects Agency and monitored by the Army Night Vision Laboratory under Contract No. DAAK 70-77-C-0082.

<sup>b)</sup>Present address: Center for Laser Studies, University of Southern California, Los Angeles, Calif. 90007.

<sup>c)</sup>California Institute of Technology, Pasadena, Calif. 91125.

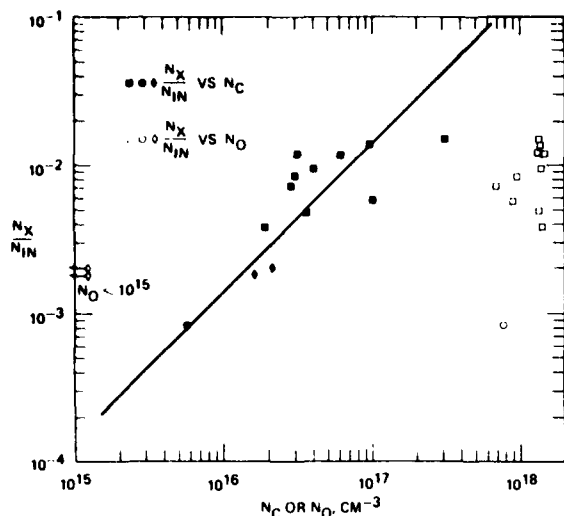


FIG. 2. Ratio of  $X$ -level concentration to In concentration versus carbon concentration (solid symbols) and oxygen concentration (open symbols). Squares and circles indicate Cz-grown samples, and diamonds indicate FZ grown samples as in Fig. 1. The line shown is the least-squares fit of the mass-action law to  $N_X/N_{In}$  versus  $N_C$ .

The oxygen calibration is derived from Ref. 11 scaled to 77 K, and the carbon calibration is from ASTM F123-74 corrected for a different baseline.

A plot of  $N_X$  versus  $N_{In}$  for various growth and anneal conditions is shown in Fig. 1. The squares are data for samples from Czochralski-grown (Cz) crystals from three sources, annealed at 650 °C for 30 min. These data, which include previously reported results,<sup>1</sup> exhibit, as before, a strong correlation between  $N_X$  and  $N_{In}$ . However, when data (circles) for similarly annealed samples from Czochralski crystals grown under different conditions are added, the scatter in the  $N_X$  versus  $N_{In}$  plot increases considerably. Data (diamonds) for 650 °C/30-min annealed samples from float-zone-grown crystals (FZ) fall both within the original group of data (squares) and well outside it.

To determine whether the scatter was introduced by variation in some other component of an In complex responsible for the  $X$  level,  $N_C$  and  $N_O$  were measured by means of ir absorption as described above for samples scattered through Fig. 1 (solid symbols). In Fig. 2 the ratio  $N_X/N_{In}$  is plotted both versus  $N_C$  (solid symbols) and  $N_O$  (open symbols).  $N_X/N_{In}$  is closely proportional to  $N_C$  over nearly two orders of magnitude but shows essentially no correlation with  $N_O$ , confirming our previous conclusion<sup>1</sup> that O is not involved in the complex.

This relation between  $N_X/N_{In}$  and  $N_C$  is identical with the mass-action law  $N_X = KN_{In}N_C$  expected if an In-C pair is the cause of the  $X$  level. A least-squares fit to the data give a value of  $(1.4 \pm 0.3) \times 10^{-19} \text{ cm}^3$  for the association constant  $K$  at 650 °C.

Annealing at 850 °C for 1 h caused large reductions in  $N_X$ . These changes were completely reversible between the 650 and the 850 °C anneal states and are shown as the paired

points in Fig. 1. Such behavior is consistent with the model of an In-C pair, since the association constant in this model has a temperature dependence:

$$K = 4\nu f \exp(E_B/kT), \quad (1)$$

where  $E_B$  is the decrease in energy upon formation of the pair,  $\nu$  is the volume per atom in the Si lattice ( $2 \times 10^{-23} \text{ cm}^3$ ), and  $f$  is a factor close to unity that is related to bond vibrational frequencies. From the temperature dependence of Eq. (1), a value for  $E_B$  of  $0.7 \pm 0.1 \text{ eV}$  can be inferred from the change in  $N_X$  between 650 and 850 °C for the four samples shown in Fig. 1. Substituting the value of  $E_B$  and the 650 and 850 °C value for  $K$  in Eq. (1), we obtain a value for  $f$  of 0.3 with an uncertainty of a factor of 4.

Such an energy decrease is to be expected when In and C form a substitutional pair in Si. Indium has a larger covalent radius<sup>13</sup> (1.44 Å) than Si (1.17 Å), while C has a smaller covalent radius (0.77 Å). Hence, an In-C substitutional pair would strain the lattice less than either a separate substitutional In or C. The largest reduction in the strain energy would occur when the atoms occupy nearest-neighbor sites. A substitutional In paired with an interstitial C is not likely to result in any strain relief. In addition, it is reasonable to expect that nearest-neighbor In and C would form a chemical bond which is stronger than that with Si.<sup>13</sup> The binding energy of the pair ( $0.7 \pm 0.1 \text{ eV}$ ) is consistent with the strain energies for the individual constituents. The strain energy of In in Si is about 0.7 eV,<sup>14</sup> while that for C in Si is about 1.4 eV.<sup>15</sup> Due to the strain relief, the binding of the pair should be less than the larger (1.4 eV) of these numbers.

The identification of the  $X$  level as the  $\text{In}_i\text{-C}_s$  pair is also consistent with the expected electronic properties of the pair. Carbon should be inactive as a substitutional dopant in Si since it comes from column IV of the periodic table. Hence, an  $\text{In}_i\text{-C}_s$  pair should act as a single acceptor. In contrast, a C interstitial paired with a substitutional In is likely to produce no electrical activity. Interstitial C is a very deep donor,<sup>17</sup> and when paired with an In acceptor should act as a donor-acceptor pair and not as a dopant.

The energy level associated with the  $X$  level is what one might expect for a nearest-neighbor In-C substitutional pair. Indium produces a potential which is made up of the Coulomb potential plus an attractive potential due to the central cell correction and the strain induced in the lattice. This potential produces a moderately deep ground-state level<sup>16</sup> at 0.157 eV and a hole wave function extending to at most a few near neighbors. Hence, for a second impurity atom to modify the ground-state energy significantly, it must be located on one of the near-neighbor lattice sites. The increase in pair binding for sites closer to In suggests that the C is on a nearest-neighbor site.

Further, the central cell correction and change in the strain potential due to the replacement of one of the nearest-neighbor Si atom by a C atom will be repulsive for holes.<sup>18</sup> The addition of this repulsive potential should decrease the ionization energy of an  $\text{In}_i\text{-C}_s$  pair compared to an isolated  $\text{In}_i$ . Hence, the fact that the observed ionization energy of the

$X$  level (0.111 eV) is significantly smaller than that of In, (0.157 eV) is consistent with the identification of the  $X$  level as an  $\text{In}_i\text{-C}_j$  nearest-neighbor pair.

In summary, we have shown that the  $X$ -level concentration follows the mass-action law for an In-C pair. Comparison of the experimental properties of the  $X$ -level with those expected for interstitial or substitutional C paired with substitutional In leads us to conclude that it is a substitutional carbon-indium pair. The identification of the  $X$ -level defect as an  $\text{In}_i\text{-C}_j$  pair indicates that consistent growth of In-doped Si with low concentrations of the  $X$ -level defect requires that the carbon concentration be kept small.

We acknowledge valuable discussions with J. Hopfield, G. Watkins, and L. Kimerling. We are grateful to J. Baker, of Dow Corning, for the samples used for calibration and reference in the infrared experiment. We also thank M.J. Sheets, D.J. O'Connor, R.A. Walker, A.F. Rabideau, M.F. Harvey, and R. Wong Quen for their skilled assistance in crystal growth and electrical and optical measurements.

<sup>1</sup>R. Baron, M.H. Young, J.K. Neeland, and O.J. Marsh, *Appl. Phys. Lett.* **30**, 594 (1977).

<sup>2</sup>J.P. Baukus, R. Baron, M.J. Sheets, and O.J. Marsh, *Proc. of the IRIS Specialty Group on Infrared Detectors*, 1978 (Infrared Information and Analysis Center, Ann Arbor, to be published).

<sup>3</sup>E.L. Kern, R. Baron, R.A. Walker, D.J. O'Connor, and O.J. Marsh, *J. Electron. Mater.* **4**, 1249 (1975).

<sup>4</sup>O.J. Marsh, Final Technical Report on Contract DAAK02-75-C-0079, U.S. Army Night Vision Laboratory, 1976 (unpublished).

<sup>5</sup>R.N. Thomas, T.T. Braggins, H.M. Hobgood, and W.J. Takei, *J. Appl. Phys.* **49**, 2811 (1978).

<sup>6</sup>R.D. Larrabee, *Semiconductor Characterization Techniques*, edited by P.A. Barnes and G.A. Rozgonyi (Electrochemical Society, Princeton, N.J., 1978), p. 71.

<sup>7</sup>W. Scott, *Appl. Phys. Lett.* **32**, 540 (1978).

<sup>8</sup>R. Baron, M.H. Young, J.K. Neeland, and O.J. Marsh, *Semiconductor Silicon 1977*, edited by H.R. Huff and E. Sirtl (Electrochemical Society, Princeton, N.J., 1977), p. 367.

<sup>9</sup>R. Baron, M.H. Young, J.P. Baukus, O.J. Marsh, and M.J. Sheets, *Proc. of the IRIS Specialty Group on Infrared Detectors*, 1977 (Infrared Information and Analysis Center, Ann Arbor, 1977), Vol. I, p. 23.

<sup>10</sup>R. Baron, M.H. Young, and J.P. Baukus (unpublished).

<sup>11</sup>W.R. Thurber, NBS Technical Note 529; ASTM F120-75; ASTM F121-76; ASTM F123-74.

<sup>12</sup>J.R. Patel, *Ref. 8*, p. 521.

<sup>13</sup>L. Pauling, *The Nature of the Chemical Bond* (Cornell U.P., Ithaca, N.Y. 1960), p. 246.

<sup>14</sup>K. Weiser, *J. Phys. Chem. Solids* **7**, 118 (1958).

<sup>15</sup>Calculated from the formula in *Ref. 14*.

<sup>16</sup>A. Baldereschi and N.O. Lipari, *Proc. of the 13th Int. Conf. of Semiconductors*, edited by L.G. Fumi (Tipografia Marves, Rome, 1977), p. 595, for the case with no central cell correction. The binding energy for In is substantially larger than the 0.070 eV found for this case.

<sup>17</sup>L.C. Kimerling, *Proc. of the Int. Conf. on Radiation Effects in Semiconductors*, 1976 (Institute of Physics and Physical Society, London, 1977), p. 221; (private communication).

<sup>18</sup>The potential for holes due to C, in Si is not known. However, boron, which comes from the same row in the periodic table as C, produces a repulsive central cell correction. The ground state of boron is 0.0457 eV, as compared to that for a coulombic center of 0.070 eV (see *Ref. 16*).

APPENDIX B

OBSERVATION OF LONG LIFETIME LINES IN  
PHOTOLUMINESCENCE FROM Si:In

# OBSERVATION OF LONG LIFETIME LINES IN PHOTOLUMINESCENCE FROM Si:In\*

G. S. Mitchard<sup>†</sup>, S. A. Lyon, K. R. Elliott and T. C. McGill  
California Institute of Technology  
Pasadena, California 91125

(Received 16 August, 1978 by H. Suhl)

We report the first observation of lines with lifetimes of about 200  $\mu$ s in silicon samples doped with indium. These long lifetimes are comparable to the radiative lifetime for the indium bound exciton and suggest that these lines are due to isoelectronic centers in silicon.

The luminescence spectra of Si:In have been the subject of a great deal of recent interest (1-4). Dean *et al* reported lines due to no-phonon (NP) and longitudinal plus transverse optical phonon (LO + TO) transitions of the ground state of the In bound exciton (BE) at 1141.3 meV and 1083.5 meV, respectively. Other workers have studied the lines due to excited states of the In BE at 1144.0 meV (3-5) and 1147.2 meV (5) in the NP transition. In the work of Lightowlers and Vouk (2) additional lines of unknown origin were observed.

In this note we report the observation of long lifetime ( $\tau \sim 200 \mu$ s) lines in Si doped with In. The long lifetimes of these lines suggest that they are due to excitons bound to isoelectronic traps.

Measurements were made on crystals grown by the float-zone and Czochralski techniques. The detailed results which will be reported here were obtained by studying a sample grown by the Czochralski technique. Hall effect measurements performed at Hughes Research Laboratories determined the indium concentra-

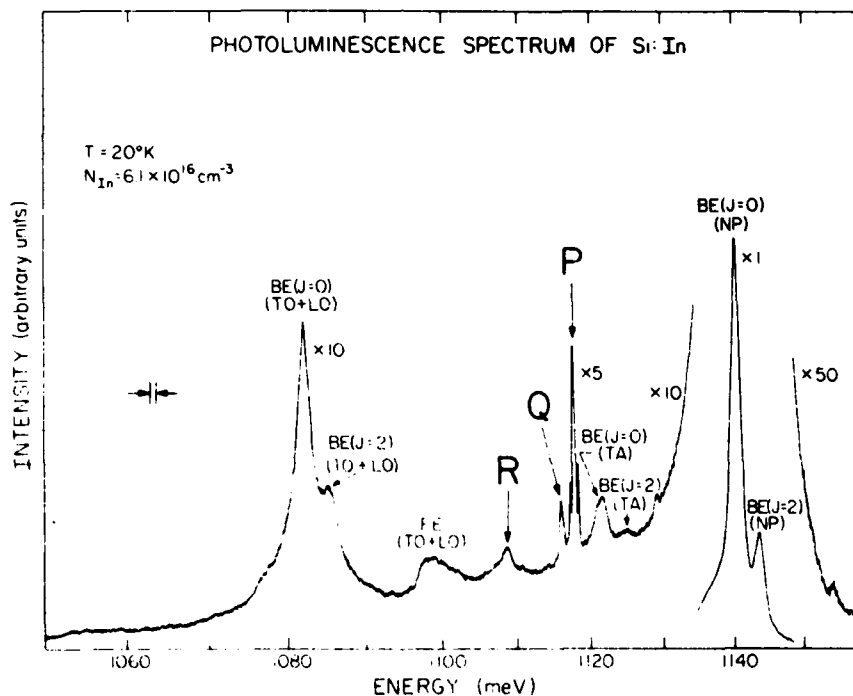


Figure 1. The photoluminescence spectrum of Si:In at 20°K. The lines labelled BE are associated with the In bound exciton, and the line labelled FE is associated with the free exciton. The lines labelled P, Q and R are the long lifetime lines discussed in the text.

<sup>†</sup> National Research Council of Canada Postgraduate Scholar

\* Research supported in part by the Advanced Research Projects Agency under Contract No. DAAK70-77-C-0087

tion in this sample to be  $6.1 \times 10^{16} \text{cm}^{-3}$ . The crystals were mechanically lapped and chemically etched to ensure smooth, damage-free surfaces, and then mounted in a Janis variable temperature cryostat.

Two excitation sources were used. The time-resolved spectra were excited by an RCA SG2004 GaAs laser diode mounted in the cryostat near the sample being measured. The peak output of this laser was about 1 watt at 8500 Å, and it was pulsed at a rate of 100 kHz with a pulse length of 4  $\mu\text{sec}$ . The spot size was estimated to be about 1 mm in diameter. The remaining spectra were excited by a Spectra-Physics Model 166 Ar<sup>+</sup> laser operated in the cw mode. The output was 1 watt and the spot size was approximately 2 mm in diameter. The luminescence was then collected from the edge of the sample, directed through the entrance slits of a Spex Model 1269 spectrometer, measured with an S-1 photomultiplier (RCA 7102) cooled to liquid nitrogen temperature, and processed with gated photon counting electronics.

A typical spectrum obtained in this manner is shown in Fig. 1. The spectrum clearly shows lines due to the BE in the NP, LO + TO and transverse acoustic phonon (TA) replicas. In addition to these lines, three lines labelled P, Q and R are also observed. Two of these lines, P and R, were previously observed by Vukobratovic and Lightowler<sup>(2)</sup> who labelled them U<sub>2</sub> and U<sub>3</sub>. The P, Q and R lines are all rather sharp and intense. The intensity of these lines is greatly reduced in samples grown by the float zone technique. Further, the lines have not been observed in any samples which were not doped with In. A number of other weak lines have also been observed in the Si:In spectrum. The positions of all the lines, along with some identifications, are listed in Table I.

Table I. The energy and assignment of some of the lines observed in the photoluminescence spectrum shown in Figure 1 for a Si:In sample.

Peak Energy, <sup>a</sup> meV	Identification
1077.6	?
1082.0	TO + LO phonon In BE (J = 0)
1085.1	TO + LO phonon In BE (J = 2)
1093.3	?
1098.4	TO + LO phonon FE
1101.1	?
1105.7	?
1108.6	R
1110.7	?
1114.4	?
1115.9	Q
1117.6	P
1121.5	TA phonon In BE (J = 0)
1125.1	TA phonon In BE (J = 2)
1129.2	?
1136.5	?
1140.3	In BE (J = 0)
1143.7	In BE (J = 2)
1154.3	?

<sup>a</sup> Energies accurate to  $\pm 0.2$  meV

We have examined the decay characteristics of the P, Q and R lines. The results at 20°K are shown in Fig. 2. The data were obtained from time resolved spectra. The pulsed GaAs laser diode was used as the excitation source, and the time resolution was accomplished by gating the output signal at the desired time after the end of the laser pulse. For measurement of the long decay times in question here, the gate width used was 20  $\mu\text{sec}$ . Since the entire time resolved spectrum was available, it was possible to subtract out the background from each point to obtain an accurate decay curve. An exponential decay of intensity with time was assumed, and the indicated lifetimes were determined from the exponential least-squares best fit to the measured data points. The most interesting information to be obtained from this figure is the exceptionally long lifetimes exhibited by these lines. At 20°K, the lifetimes measured for lines P, Q and R are  $196 \pm 5$   $\mu\text{sec}$ ,  $170 \pm 14$   $\mu\text{sec}$ , and  $220 \pm 29$   $\mu\text{sec}$ , respectively.

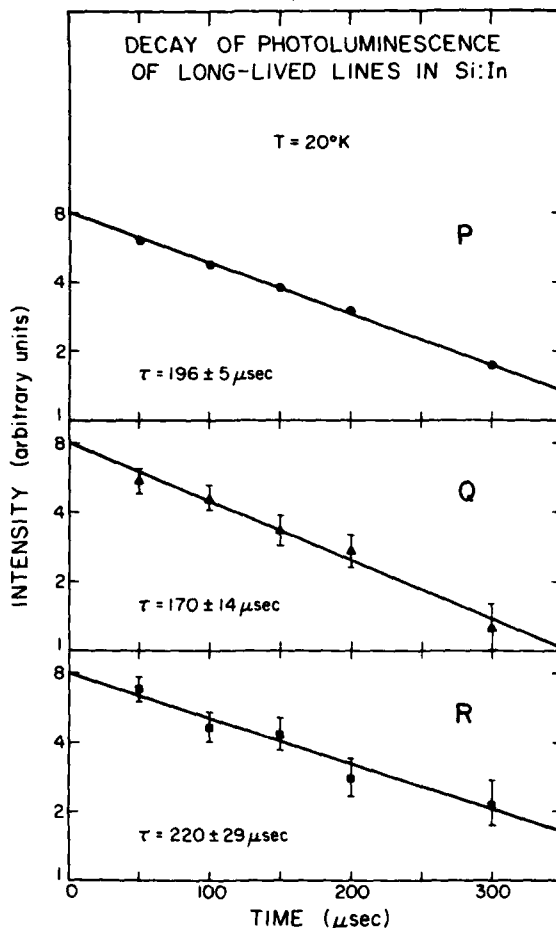


Figure 2. Typical decay curves for the long lifetime lines in Si:In, at 20°K. The intensities were normalized to the same value at zero seconds. The slopes are inversely proportional to the lifetimes, which are given on the figure.

The temperature dependence of these lines has also been investigated. In Fig. 3, spectra taken at various temperatures from 5°K to 25°K are shown. For purposes of comparison, in these spectra the indium bound exciton intensity has been set to 1. These spectra show that line Q is present only at relatively high temperatures. Its intensity becomes appreciable at 15°K and increases with increasing temperature. Measurements of the intensity ratios as functions of the reciprocal of the temperature show that the ratio R/P is independent of temperature,

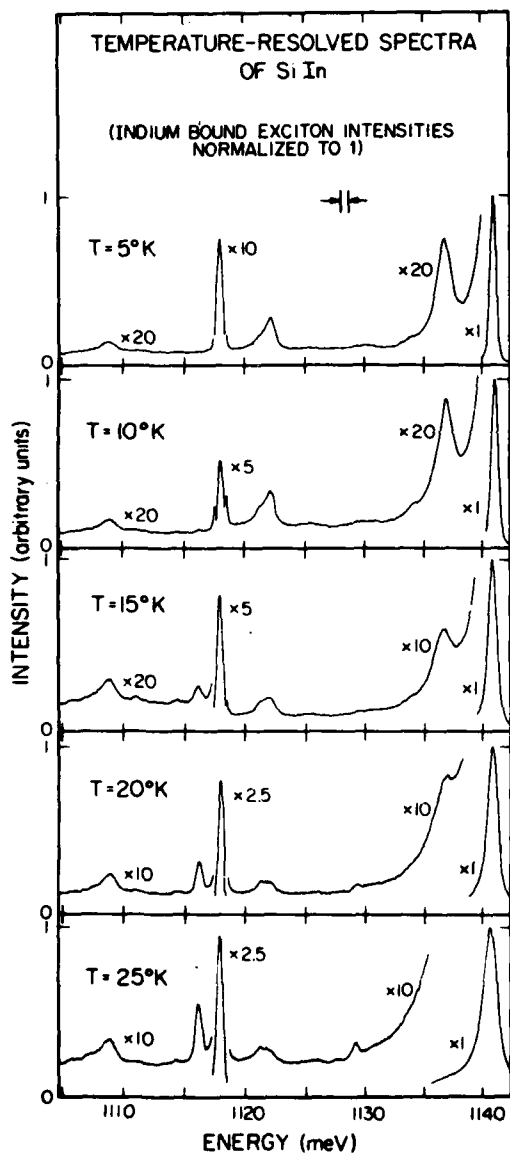


Figure 3. Photoluminescence spectra of Si:In, taken at temperatures from 5°K to 25°K. In each spectrum, the In bound exciton intensity has been normalized to 1. Note that line Q appears only at higher temperatures.

the ratio Q/P decreases with reciprocal temperature, and the ratio R/Q increases with reciprocal temperature. However, none of these ratios vary as the Boltzmann factor ( $e^{-\Delta E/kT}$ , where  $\Delta E$  is the splitting between the lines). This result indicates that no pair of lines is the result of transitions from different initial states of the same center.

The decay times are found to be temperature dependent for temperatures greater than about 5°K. One possible origin of decay time temperature dependence is the ionization of the pair or of a single carrier off the center. If we assume that radiative decay,  $\tau_r$ , and ionization,  $\tau_i$ , are the two decay processes, then the measured decay time  $\tau_m$  is given by

$$\frac{1}{\tau_m} = \frac{1}{\tau_r} + \frac{1}{\tau_i} \quad (1)$$

At high temperatures, where ionization is more likely than radiative decay, then

$$\tau_m \approx \tau_i \quad (2)$$

Since

$$\tau_i \approx A \left( \frac{1}{kT} \right)^2 e^{E_B/kT} \quad (3)$$

where  $E_B$  is the binding energy (6), then a plot of  $\tau_m(kT)^2$  versus the reciprocal of temperature should give a straight line with slope  $E_B$ . In Fig. 4 we have plotted  $\tau_m(kT)^2$  versus the reciprocal of temperature. The data show the expected straight line variation at high temperature yielding values of  $E_B$  of  $30 \pm 2$  meV,  $29 \pm 2$  meV and  $30 \pm 2$  meV for lines P, Q and R, respectively. These values of  $E_B$  are substantially less than those obtained by assuming that the observed lines are due to a NP transition to the ground state and then by subtracting their position from the free exciton threshold. The values obtained by this method are 37.2 meV, 39.0 meV and 46.3 meV for lines P, Q and R, respectively. One possible explanation for this effect, originally proposed by Trumbore *et al.* (7), is that a single carrier is ionized and that the difference between the thermodynamically and spectroscopically measured binding is due to the fact that the remaining carrier is left on the center during the ionization process. This suggestion may explain our results. Of course, a second possible explanation is that the cross section for capture exhibits a rapid variation with temperature.

As the temperature is decreased, the decay times are observed to go through a maximum and then decrease, becoming virtually temperature independent below about 5°K. These maximum lifetimes are different for each line, indicating that each of the P, Q and R lines are due to transitions from different initial states. The decrease in lifetime at lower temperatures seems to suggest that there are two states involved in each case; a lower energy state which has the observed low temperature lifetime, and a higher energy excited state which has a somewhat longer lifetime. However, these excited states have not been observed.

In summary, we have observed three long lifetime lines in Si:In samples. These lines have different decay times, which are all ap-

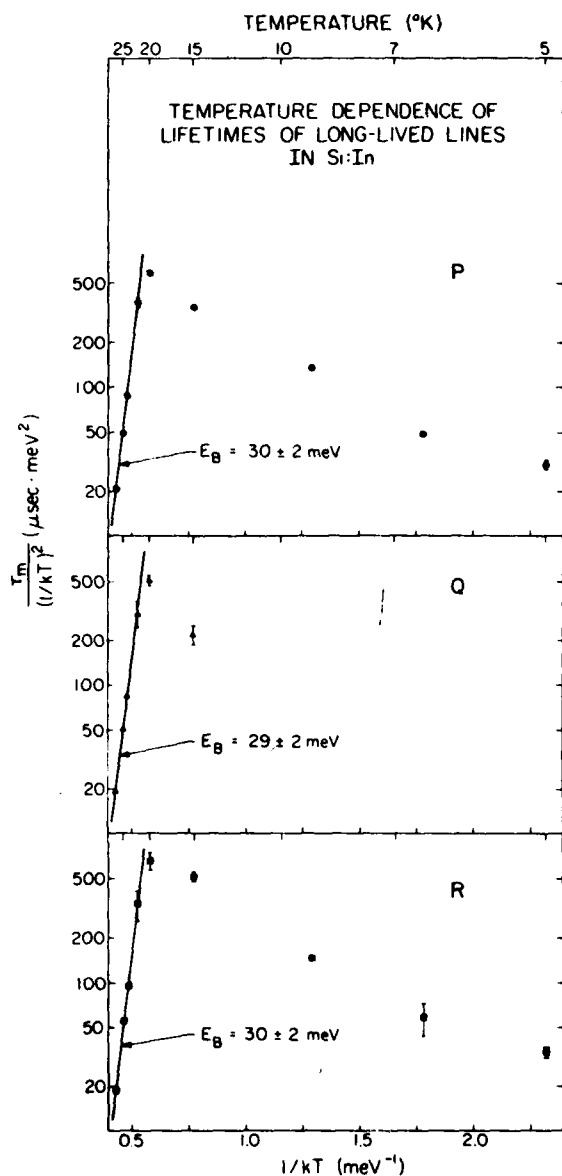


Figure 4. The temperature dependence of the lifetimes of the long lifetime lines in Si:In. We plot the lifetimes divided by  $(1/kT)^2$  in order to exhibit the thermalization at high temperatures. The binding energies calculated in this way are given on the figure.

proximately 200  $\mu\text{s}$  at 20°K. The temperature dependence of the ratios of intensity and the differences in the decay times indicate that the lines are all due to transitions from initial states on different centers. The long decay times suggest that these centers are isoelectronic traps, which decay radiatively. Centers which have a free carrier in addition to the BE decay predominantly by the Auger process and have decay times at least three orders of magnitude smaller than those observed. For example, the decay time for excitons bound to neutral donors and acceptors in silicon ranges between  $\sim 1 \mu\text{s}$  for Si:Li to 3 ns for Si:In (8,9).

The difference between the ionization energy measured thermodynamically and spectroscopically is also characteristic of an isoelectronic center (7) where the binding of one of the carriers to the center is greater than the free exciton binding energy. The precise nature of the isoelectronic centers is as yet unknown. The lines observed here cannot be directly due to the recently observed X-level since this center acts as an acceptor (10). Also, these lines do not appear to be associated with the isoelectronic trap involving carbon in silicon which has been recently observed by Weber *et al* (11). The lines they observe occur at different energies than lines P, Q and R. The fact that we have only observed these lines in samples doped with In suggests that these centers involve In. Further, the observation that the P, Q and R lines are much stronger in Czochralski than in float-zone samples suggests that the centers may involve carbon or oxygen. We are currently studying the influence of carbon and oxygen on the concentration of these centers.

Acknowledgement- The authors gratefully acknowledge J. Baukus and R. Baron of the Hughes Research Laboratories for providing us with samples of silicon doped with indium. The authors have profited greatly from fruitful discussions with A. Hunter, G. Osbourn and D. L. Smith.

## REFERENCES

1. P. J. Dean, J. R. Haynes, and W. F. Flood, *Phys. Rev.* **161**, 711 (1967).
2. M. A. Vouk and E. C. Lightowers, *J. Luminesc.* **15**, 357 (1977).
3. M. A. Vouk and E. C. Lightowers, Proceedings of the Thirteenth International Conference on the Physics of Semiconductors, Rome, 1976, edited by F. G. Fumi, (Tipografia Marves, Rome, 1977), p. 1098.
4. S. A. Lyon, D. L. Smith, and T. C. McGill, *Phys. Rev. B* **17**, 2620 (1978).
5. K. R. Elliott, G. C. Osbourn, D. L. Smith, and T. C. McGill, *Phys. Rev. B* **17**, 1808 (1978).
6. This result comes from the application of detailed balance assuming a temperature independent capture cross section. The density of states varies as  $T^{3/2}$  and the thermal velocity varies as  $T^{1/2}$  yielding the  $T^2$  dependence.
7. F. A. Trumbore, M. Gershenson, and D. G. Thomas, *Appl. Phys. Lett.* **9**, 4 (1966).
8. S. A. Lyon, G. C. Osbourn, D. L. Smith, and T. C. McGill, *Solid State Comm.* **23**, 425 (1977).
9. W. Schmid, *Phys. Stat. Solidi* **b84**, 529 (1977).
10. R. Baron, M. H. Young, J. K. Neeland, and O. J. Marsh, *Appl. Phys. Lett.* **30**, 594 (1977).
11. J. Weber, W. Schmid, and R. Sauer, Proceedings of the International Conference on Luminescence, Paris, 1978 (to be published).

APPENDIX C

EVIDENCE FOR AN EXCITED LEVEL OF THE NEUTRAL  
INDIUM ACCEPTOR IN SILICON

EVIDENCE FOR AN EXCITED LEVEL OF THE NEUTRAL INDIUM ACCEPTOR IN SILICON<sup>\*</sup>

K.R. ELLIOTT, S.A. LYON, D.L. SMITH and T.C. MCGILL

*California Institute of Technology, Pasadena, CA 91125, USA*

Received 27 September 1978

On the basis of the dependence of the photoluminescence on pump power, indium concentration and temperature we have determined that an excited level of the neutral indium acceptor exists  $4.1 \pm 0.1$  meV above the ground state.

Studies of the luminescence of semiconductors are valuable in understanding the properties of impurities in these materials. Recently Lyon et al. [1] and Vouk et al. [2] reported studies of the luminescence in Si:In. In addition to previously observed transitions such as the bound exciton, these studies reported several new transitions, one of which is approximately 4 meV lower in energy than the principal bound exciton transition. (Following Vouk et al. [2] we will refer to this line as U1.) Neither Lyon et al. nor Vouk et al. suggested an origin for the line. Vouk et al. did mention that the feature appeared to increase in intensity relative to the bound exciton with increasing temperature. We have investigated the change in intensity of U1 relative to the bound exciton as a function of pump power, doping level and temperature. These measurements suggest that U1 and the bound exciton transition have the same initial state. The difference in energy between the two final states matches that of an excited level of the neutral indium acceptor indirectly observed in ultrasonic attenuation experiments [3]. Spectra were obtained from four different samples doped with Si:In. The impurity concentration was determined in each of these with a Hall measurement performed at Hughes Research Laboratories and was found to be  $2 \times 10^{14} \text{ cm}^{-3}$ ,  $3.2 \times 10^{15} \text{ cm}^{-3}$ ,  $1.7 \times 10^{16} \text{ cm}^{-3}$  and  $2 \times 10^{17} \text{ cm}^{-3}$ . Optical excitation was provided by a rhodamine 6G dye laser at 6000 Å. The sample was placed in a variable temperature dewar

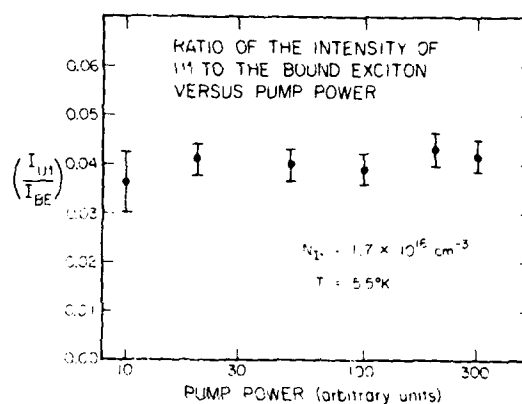


Fig. 1. Ratio of the intensity of U1 to the bound exciton versus pump. The absolute pump power ranged approximately from 100 mW/cm<sup>2</sup> to 3000 mW/cm<sup>2</sup>.

and the temperature was monitored with a silicon diode sensor mounted directly on the sample. The photoluminescence was passed through a grating monochromator and monitored with a cooled S-1 photomultiplier and photon counting system.

Figs. 1, 2, and 3 show the ratio of U1 to the bound exciton as a function of pump power, doping level, and temperature, respectively. The fact that the ratio is independent of pump power and doping level establishes that the line is not due to a multiple exciton complex. Such lines are observed to increase in intensity with pump power and decrease in intensity at higher doping levels with respect to the bound exciton. Fig. 3 shows that the ratio of U1 to the bound exciton is independent of temperature up to 15 K. There is al-

<sup>\*</sup> Work supported in part by Advanced Research Projects Agency under contract no. DAAK70-77-C-0082.

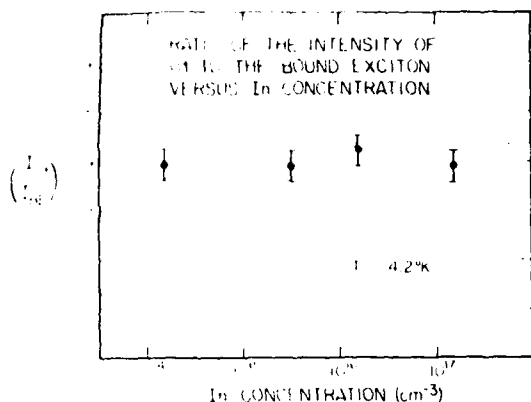


Fig. 2. Ratio of the intensity of U1 to the bound exciton as a function of indium concentration.

ways a background present on the low energy tail of the bound exciton, however, which increases at higher doping levels and higher temperature. It is thus necessary to subtract this background to obtain a reliable estimate of the ratio. Above 15 K the background dominates as the width of the bound exciton increases, and it is not possible to obtain a reliable estimate. The peak height of the bound exciton also decreases rapidly above 15 K as the line broadens, and thus it is important that one uses the integrated intensity in determining the ratio.

In view of the temperature and concentration dependence of the data it is unlikely that U1 is due to

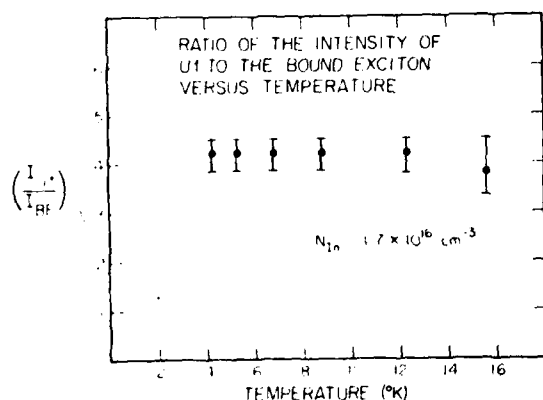


Fig. 3. Ratio of the intensity of U1 to the bound exciton as a function of temperature. The excitation intensity was approximately 1000 mW/cm<sup>2</sup>.

the recombination of a bound exciton on a site other than a substitutional indium. In such a case one would expect some temperature dependence to the ratio since the capture cross section of an exciton on an isolated indium site is relatively sensitive to temperature [4]. In addition the samples used in this experiment had different past histories. Some were grown using a float zone technique; whereas others were grown by the Czochralski method. In all cases the same ratio was obtained for the intensity of U1 to the BE. We therefore conclude that the transition U1 has the same initial state as the bound exciton transition.

It is possible that the energy difference between U1 and the bound exciton is due to the creation of a resonant phonon mode upon recombination. However, the mass defect between an indium atom and a silicon atom is roughly a factor of 4 and on the basis of this we would estimate any resonant mode to have an energy between 20 and 30 meV.

We think that a more likely explanation is that the final state of the U1 transition is an excited level of the indium acceptor. In fact an excited level of the neutral indium acceptor  $4.2 \pm 0.3$  meV above the ground has recently been indirectly detected in ultrasonic attenuation experiments performed by Schad et al. [3] in Si:In samples as compared to the value  $4.1 \pm 0.1$  meV measured in our experiments. They suggested that the dynamic Jahn-Teller effect might play a role in producing the level they detected. In addition, Morgan [5] has pointed out that the dynamic Jahn-Teller effect should have important consequences for acceptor states with  $\Gamma_8$  symmetry. The effect on the indium acceptor should be particularly pronounced since it is considerably deeper than all the group III elements except for thallium and the hole wavefunction is highly localized near the impurity. For sufficiently strong vibronic coupling there will be bands of levels produced as a result of the dynamic Jahn-Teller effect. Evidence that the effect is important is given by the anomalously large stress dependence in the  $g$  factors and resonance linewidths of holes bound to acceptors in Si [6]. Morgan suggested that these data could be explained by the dynamic Jahn-Teller effect [5]. Thus it is reasonable to assume that the dynamic Jahn-Teller effect may be playing a role here also. Further experiments and theory to test this assumption is a topic for further research.

In conclusion we have determined that there is an energy level  $4.1 \pm 0.1$  meV above the indium neutral acceptor ground state from measurements of the Si:In luminescence as a function of pump power, doping level and temperature.

The authors gratefully acknowledge R. Baron and J. Baukus of the Hughes Research Laboratory for providing the samples of In doped Si used in this study.

#### References

- [1] S.A. Lyon, D.L. Smith and T.C. McGill, *Phys. Rev.* B17 (1978) 2620.
- [2] M.A. Vouk and E.C. Lightowers, *J. Luminescence* 15 (1977) 357.
- [3] Hp. Schad and K. Lassmann, *Phys. Lett.* 56A (1976) 409.
- [4] K.R. Elliott, D.L. Smith and T.C. McGill, *Solid State Commun.* 24 (1977) 461.
- [5] T.W. Morgan, *Phys. Rev. Lett.* 24 (1970) 887.
- [6] G. Feher, J.C. Hensel and E.A. Gere, *Phys. Rev. Lett.* 5 (1960) 309.